Geological Quarterly, 2025, 69, 46
DOI: https://doi.org/10.7306/gq.1819

Assessment of the impact of rainfall on landslide activity in the Polish Carpathians over a decadal period

Bartłomiej WARMUZ[1, *]

[7] Polish Geological Institute – National Research Institute, Skrzatów 1, 31-560 Kraków, Poland; ORCID: 0000-0001-9553-925X

Warmuz, B., 2025. Assessment of the impact of rainfall on landslide activity in the Polish Carpathians over a decadal period. Geological Quarterly, **69**, 46; https://doi.org/10.7306/gq.1819

This study analyses the impact of precipitation on groundwater level fluctuations and the activity of six landslides in the Polish Flysch Carpathians, using monitoring data from the Landslide Protection System project, including inclinometer measurements, rainfall records, and groundwater levels in colluvial deposits. Geodetic surveys of reference points installed on the landslides were also used to assess their activity. Selected measurement intervals were examined to identify rainfall conditions triggering landslide movement. Cumulative displacement curves revealed nearly continuous movement, with velocities ranging from 0.3 to 3 mm/month. Displacement values causing inclinometer column shearing varied from 38 mm (Witanowice) to 232 mm (Ruszelczyce), depending on shear zone thickness and rock plasticity. Acceleration typically occurred during prolonged rainfall, especially when monthly totals exceeded 100 mm. However, defining a precise rainfall threshold and timing of acceleration was difficult due to complex geological conditions, irregular precipitation patterns, and limited measurement frequency. The findings highlight the sensitivity of landslide activity to hydrological changes and emphasize the need for frequent, integrated monitoring to better understand and predict slope instability in flysch terrains.

Key words: Landslides, mass movements, Flysch Carpathians, inclinometric monitoring, rainfall thresholds.

INTRODUCTION

The landslides described in this article are located in southern Poland, within the Outer Flysch Carpathians (Fig. 1A). This region is characterized by uplands and low mountain ranges, featuring dispersed settlements, a dense road network, and relatively high population density. Landslides, which constitute one of the primary natural hazards in this area, exert a significant influence on land use planning and spatial development (Cała, 2009; Wójcik and Wojciechowski, 2016; Perski et al., 2019).

In the Flysch Carpathians, the most common trigger for landslide activation is intense rainfall (Ziętara, 1974; Starkel, 1996; Gil, 1997). The question of the minimum duration and intensity of rainfall capable of triggering shallow landslides was first addressed by Caine (1980). Since then, various rainfall thresholds have been proposed for numerous regions, as comprehensively reviewed by Guzzetti et al. (2008). The dependence of landslide activity on hydrometeorological conditions in the Carpathians has been examined in several studies (Gil, 1997; Gil and Długosz, 2006; Gil et al., 2009). The effects of precipitation infiltration and the resulting changes in groundwater levels were analysed as causes of increased pore water pressure leading to the reactivation of several landslides in the Beskid Niski mountain range (Zabuski et al., 2004; Mrozek et al., 2006; Bednarczyk, 2015). Warmuz and Nescieruk (2019) demonstrated, using examples from several Carpathian landslides, that rainfall events with similar magnitudes and temporal distributions can yield markedly different landslide responses. This variability is primarily controlled by the filtration (permeability) properties of the colluvial deposits.

Perski and Wojciechowski (2022) described correlations between landslide activity and atmospheric precipitation for several Carpathian sites. Their study employed the InSAR method, leveraging radar backscatter from artificial reflectors installed on the landslides.

Given the rock-soil mass heterogeneity, complex geology and hydrogeology, and limited site data, linking rainfall to landslide activity is challenging. To address this objective, I conducted analyses of the effects of atmospheric precipitation on groundwater level fluctuations and on landslide displacement rates. Comparable studies have been carried out previously, aiming to estimate rainfall totals and durations in order to define so-called rainfall thresholds that initiate landslide movement in the Flysch Carpathians (Thiel, 1989; Starkel, 1996; Gil, 1997; Rączkowski and Mrozek, 2002; Gorczyca, 2004; Gil and Długosz, 2006; Zabuski et al., 2009). However, these studies employed datasets covering a time span ranging from several months to two years.

This article draws on monitoring data for landslides threatening infrastructure, collected within the Landslide Protection System project, whose overarching goal is to reduce landslide risk in Poland (Grabowski and Przybycin, 2010; Marciniec et al.,

* E-mail: bartlomiej.warmuz@pgi.gov.pl

Received: September 8, 2025; accepted: October 28, 2025; first published online: December 20, 2025

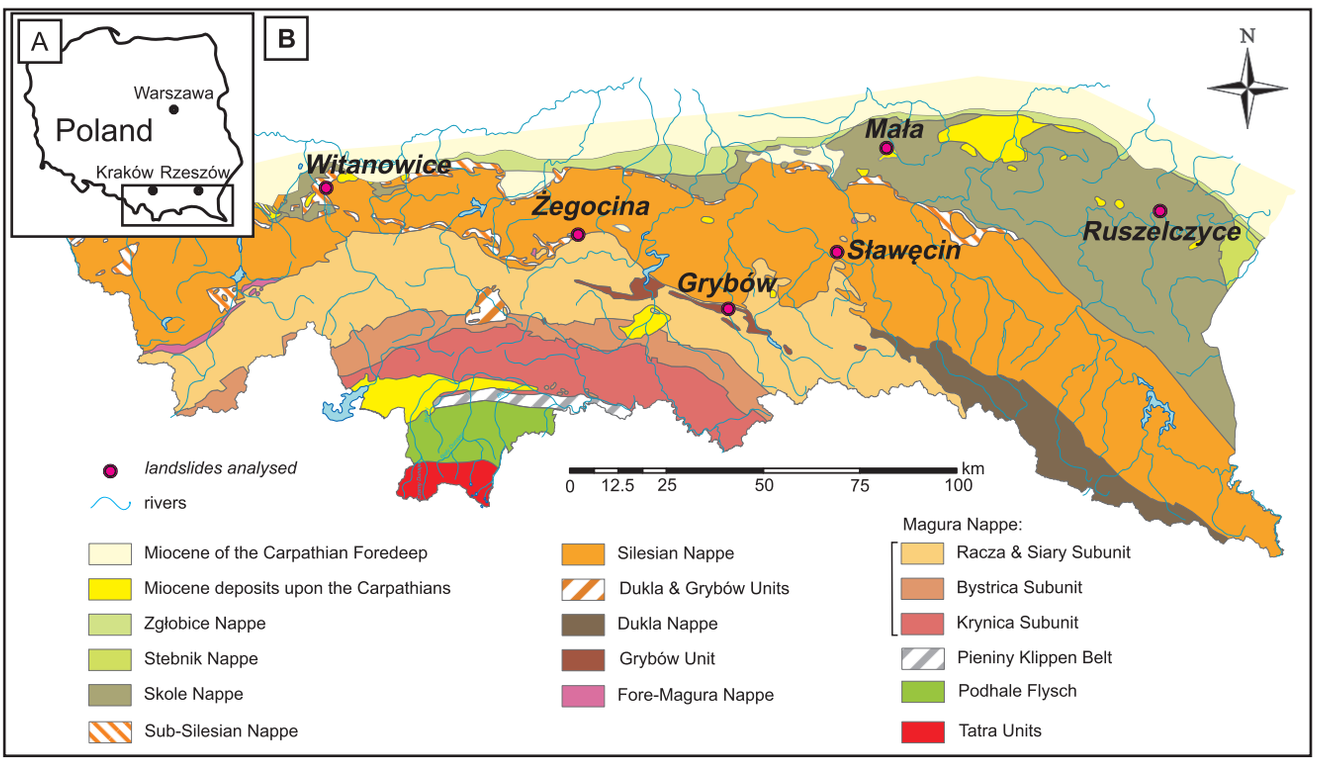

Fig. 1A – location of the study area, B – landslide locations on the Geological Map of the Polish Carpathians (Żytko et al., 1989, modified)

2015, 2019; Wójcik et al., 2020). The monitoring focuses primarily on landslides in the southern part of the country (Warmuz and Nescieruk, 2019). This study analyses 6 out of more than 60 such landslides.

This study explores the influence of atmospheric precipitation on changes in the activity of landslides composed predominantly of clay shale-rich flysch strata. The integration of long-term data on precipitation, groundwater level fluctuations, and ground deformation enables a more comprehensive understanding of landslide processes. Establishing a model of landslide activity serves as a foundation for forecasting future landslide hazards (Wójcik et al., 2020).

GEOLOGICAL SETTING

Geologically, the landslides investigated are situated within the Sub-Silesian, Silesian, Skole, and Magura tectonic nappes of the Outer Flysch Carpathians (Fig. 1B). The landslide in the village of Mała is located partly within Miocene transgressive deposits overlying flysch rocks. Basic information on the locations of the landslides described in this article is shown in Table 1, while their detailed characteristics are provided later in the text.

The Carpathians flysch are composed of terrigenous marine strata ranging in age from the Upper Jurassic to the Lower Miocene (Książkiewicz, 1953; Nowak, 1973; Golonka et al., 2008). A defining feature of the Carpathian Flysch is the alternating succession of sandstones, conglomerates, siltstones, and claystones/mudstones, with variable proportions across lithostratigraphic units. These rocks are folded, fractured, and dissected by faults. The flysch successions are subdivided into a series of tectonic units thrust northwards over one another.

Slope mantles consist of silty and clayey colluvium that grades at depth into a typical weathering profile. These are low-permeability soils (Pazdro and Kozerski, 1990) with thicknesses of up to several metres. Based on field investigations near Gorlice, Zydroń et al. (2015) obtained hydraulic conductivity values ranging from 5.7×10^{-7} to 6.5×10^{-5} m/s, whereas laboratory test results reported in the same study were significantly lower by up to three orders of magnitude. On the landslides described here, colluvial deposits exhibit better filtration (permeability) properties than do the deeper clay shales, which are commonly classified as effectively impermeable rocks (Pazdro and Kozerski, 1990).

The first landslide described in this article is located in the village of Witanowice on the right bank of the Skawa River. The landslide area is used primarily for agriculture; however, several buildings and a local road lie within its bounds. These buildings were damaged in 2010, when a marked increase in landslide activity was triggered by very intense rainfall. The relationship between this landslide's activity and precipitation was examined by Warmuz and Nescieruk (2019), who documented nearly continuous deformation that was difficult to correlate with rainfall and groundwater-level fluctuations.

In the northern part of the landslide, the bedrock comprises strata referred to as the Cieszyn Beds, consisting of black shales interbedded with fine-grained, thin-bedded sandstones (Ryłko and Paul, 2014). The substrate in the southeastern part is formed by Lower Cretaceous, coarse-grained, calcareous sandstones, medium- to thick-bedded, known as the Grodziszcze Beds (Fig. 2A).

Table 1

Landslide locations and their basic parameters

Name of landslide	Geographic coordinates of landslide center	Macroregion Mesoregion (Solon et al., 2018)	Tectonic unit	Landslide area [km^2]	Avg. slope angle of the landslide [°]	Length Width Span [m]
Witanowice	19°30'46.8" 49°54'32.1"	Pogórze Zachodniobeskidzkie Pogórze Wielickie	Silesian Nappe	0.215	7	510 540 55
Żegocina	20°25'11.6" 49°47'49.6"	Beskidy Zachodnie Beskid Wyspowy	Magura Nappe	0.019	16	200 130 60
Grybów (two-landslide complex)	20°57'29.5" 49°38'07.8"/ 20°57'16.1" 49°38'04.4"	Pogórze Środkowobeskidzkie Pogórze Rożnowskie	Magura Nappe	0.194/0.063	10	740 / 620 420 / 200 137 / 120
Sławęcin	21°20'54.0" 49°44'50.9"	Pogórze Środkowobeskidzkie Obniżenie Gorlickie	Magura Nappe / Silesian Nappe	0.185	8	700 410 92
Mała	21°31'48.9" 49°58'03.7"	Pogórze Środkowobeskidzkie Pogórze Strzyżowskie	Skole Nappe / Miocene post-orogenic deposits	0.096	7	390 280 54
Ruszelczyce	22°30'43.7" 49°49'01.3"	Pogórze Środkowobeskidzkie Pogórze Dynowskie	skolska	1.390	5	1430 1480 125

Another landslide at Żegocina occupies a relatively small area of 0.019 km^2. Currently it is scarcely visible in the field; however, after its reactivation in 2010 its boundary was delineated by a low, steep scarp and ground fissures. At that time a local road within the slide zone was destroyed. Beneath the landslide, at a depth of ~20 m, a gas pipeline runs, having been installed by horizontal directional drilling below the slip surface.

The landslide developed within sub-Magura strata referred to as the Zembrzyce shales (Wójcik et al., 2017). The lithologies involved comprise predominantly mud shales, marls and glauconitic sandstones. They occur in alternating packages several tens of centimetres thick. The stream channel immediately downstream of the landslide is underlain by a fault that separates this unit from the Wątkowa Sandstone Member (Fig. 3A).

The next study area comprises two adjacent landslides in Grybów, separated by a narrow, stable strip of slope. The landslide boundaries are complex, and the main scarps vary in height from several to over ten metres (Fig. 4B). Within the landslide zones there are twenty buildings and a network of local roads. The activity of these landslides poses a threat to these structures and may lead to uncontrolled constriction of the Biała River channel.

The landslides in Grybów are situated within the Magura nappe, bounded by rocks of the Silesian nappe. The Biała River channel downstream of the landslides is underlain by a tectonic fault (Fig. 4A). The oldest rocks in the landslide substrate consist of thin-bedded shales, marls and sandstones assigned to the Inoceramian beds. Overlying these strata is a succession of variegated shales and mudstones dated to the Paleocene–Eocene (Paul, 1993). The landslides studied occur predominantly within the variegated shales, which were encountered in all three inclinometer boreholes. The northern rim of the landslides is formed by the Ciężkowice Sandstones, chiefly coarse-grained, medium- to thick-bedded sandstones (Bromowicz et al., 1976; Leszczyński, 1981).

The next focus of investigation is the landslide at Sławęcin. It induces slow yet continuous damage to the strategic road No. 28. Several tens of buildings are also situated within the slide area (Fig. 5B).

The geological structure of this area is complex. In the upper part of the slope, variegated shales, hieroglyphic beds and the Duląbka Formation occur (Szymakowska, 1966). These rocks, belonging to the Magura Nappe, show a pronounced dominance of shales over sandstones. The middle and lower slope sections are composed of the Lower Krosno Beds of the Silesian Nappe (Wójcik et al., 1993). These consist chiefly of calcareous, muscovite-bearing shales, sporadically interbedded with thin layers of fine-grained shelly sandstone. Within the landslide limits, the tectonic thrust zone likely runs through its upper sector (Fig. 5A).

The landslide in Mała develops under particular geological conditions, with Miocene transgressive deposits overlying the Carpathian Flysch. It was initiated by a main scarp of arcuate planform reaching up to 10 m in height. At the scarp foot a depression has formed that retains water after rainfall. Two buildings are situated within the landslide mass, and a local road traverses its western sector (Fig. 6B). Evidence of landslide activity includes frequent cracking and deformation of this road's surface.

The upper part of the landslide at Mała is situated within Inoceramian Beds (Fig. 6A). These comprise thin-bedded

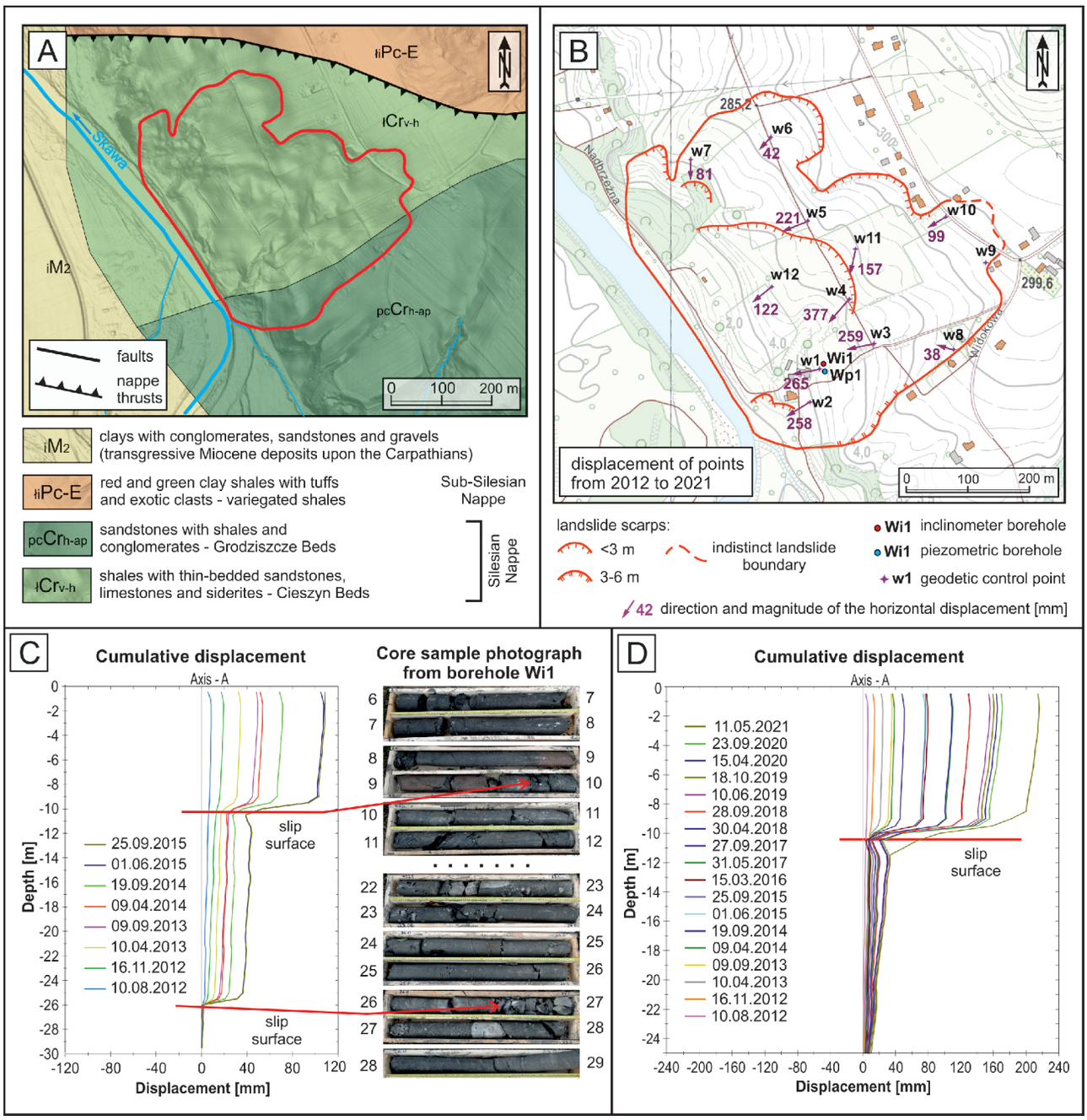

Fig. 2. Witanowice landslide

A – geological map superimposed on a digital elevation model – DEM (after Ryłko and Paul, 2014); **B** – deployment of geodetic control points on the landslide; **C** – displacement graph for inclinometer Wi1 and core sample photograph; **D** – displacements recorded by inclinometer Wi1 along the shallow slip surface

shales and sandstones together with grey marls. Shales predominate, whereas fine-grained glauconitic sandstones typically occur as thin beds. The lower slope is composed of claystones with intercalated sandstones, siltstones, and gypsum. These Miocene transgressive deposits form isolated lenses within the valleys of nearby rivers.

The final landslide described here, at Ruszelczyce, occupies a gently dipping slope on the left-bank side of the San Valley (Fig. 7B). The landslide extends over nearly 1.4 km^2, and its mean slope angle does not exceed 5°. The affected area comprises arable fields, meadows, and forested patches. In the lower sector, ~60 buildings are served by local roads, and electrical distribution lines traverse the landslide mass.

The Ruszelczyce landslide belong to a group of slides in that sector of the Carpathians characterized in terms of general geological and geomorphological aspects by Wójcik and Zimnal (1996). It was also investigated as regards the geotechnical conditions within its boundaries. At that time, it was classified as a typical subsequent landslide (Bober et al., 1997).

The complex geological structure of the landslide results from the lithological variability and a tectonic thrust zone. The oldest rocks in the landslide substrate are thin-bedded, fine-

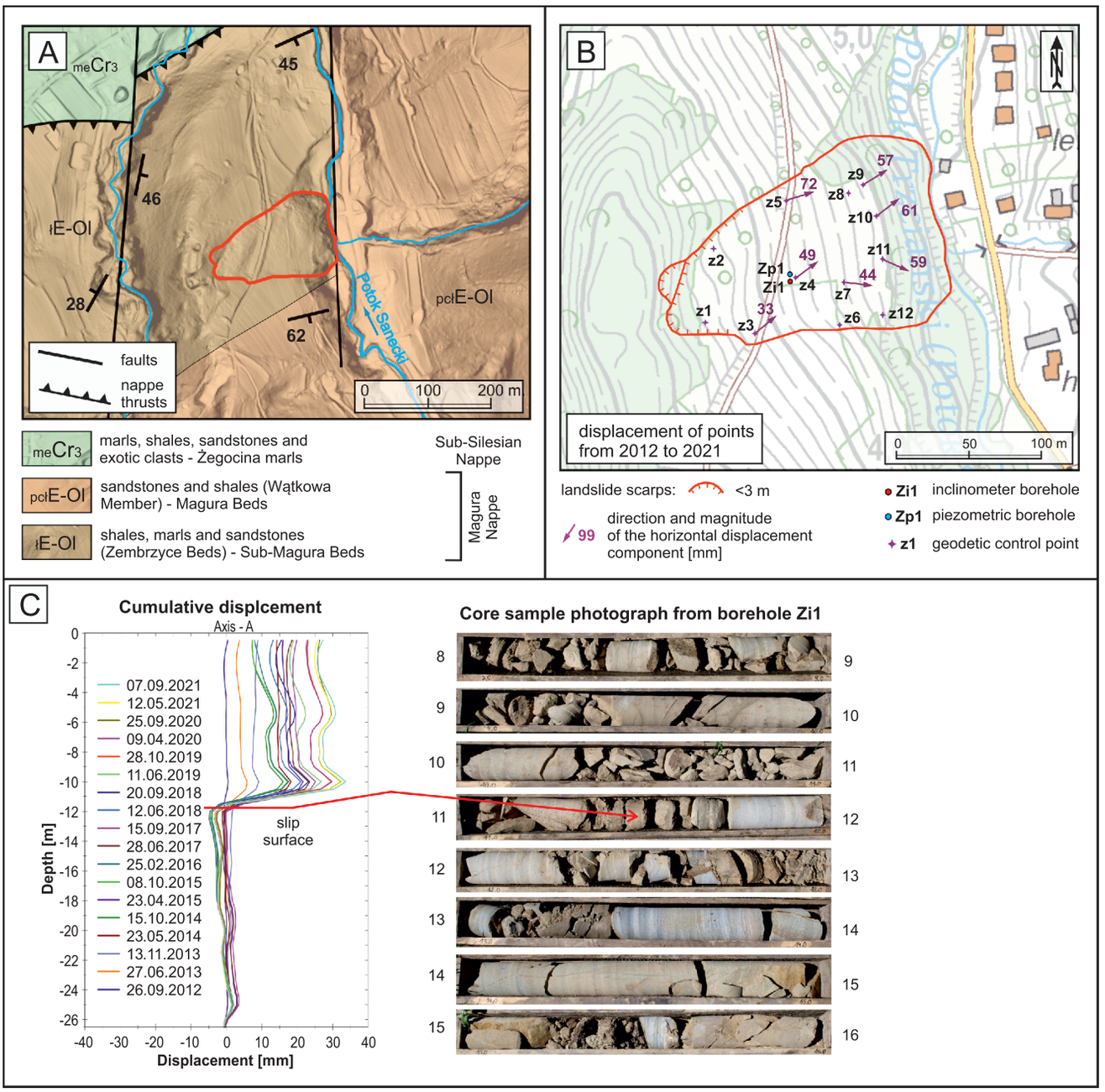

Fig. 3. Żegocina landslide

A – geological map superimposed on a DEM (after Wójcik et al., 2016); **B** – deployment of geodetic control points on the landslide; **C** – displacement graph for inclinometer Zi1 and core sample photograph

grained sandstones with intercalations of marls and variegated shales, assigned to the Inoceramian Beds. These units crop out in the eastern and western sectors of the landslide, where they are thrust over younger Menilite Formation deposits in the central sector. There, shales and marls of the Menilite strata occur. This highly tectonically disturbed succession is tightly folded, with variegated shales forming the axial part of a syncline (Fig. 7A). Variegated shales were documented in both boreholes drilled for the purpose of establishing landslide monitoring.

METHODOLOGY

From among several tens of landslides monitored under the Landslide Protection System project in the Flysch Carpathians, six were selected that exhibited slow displacements and for which complete datasets were available throughout the monitoring period.

The monitoring system comprises three components:

– subsurface monitoring based on inclinometer measurements;

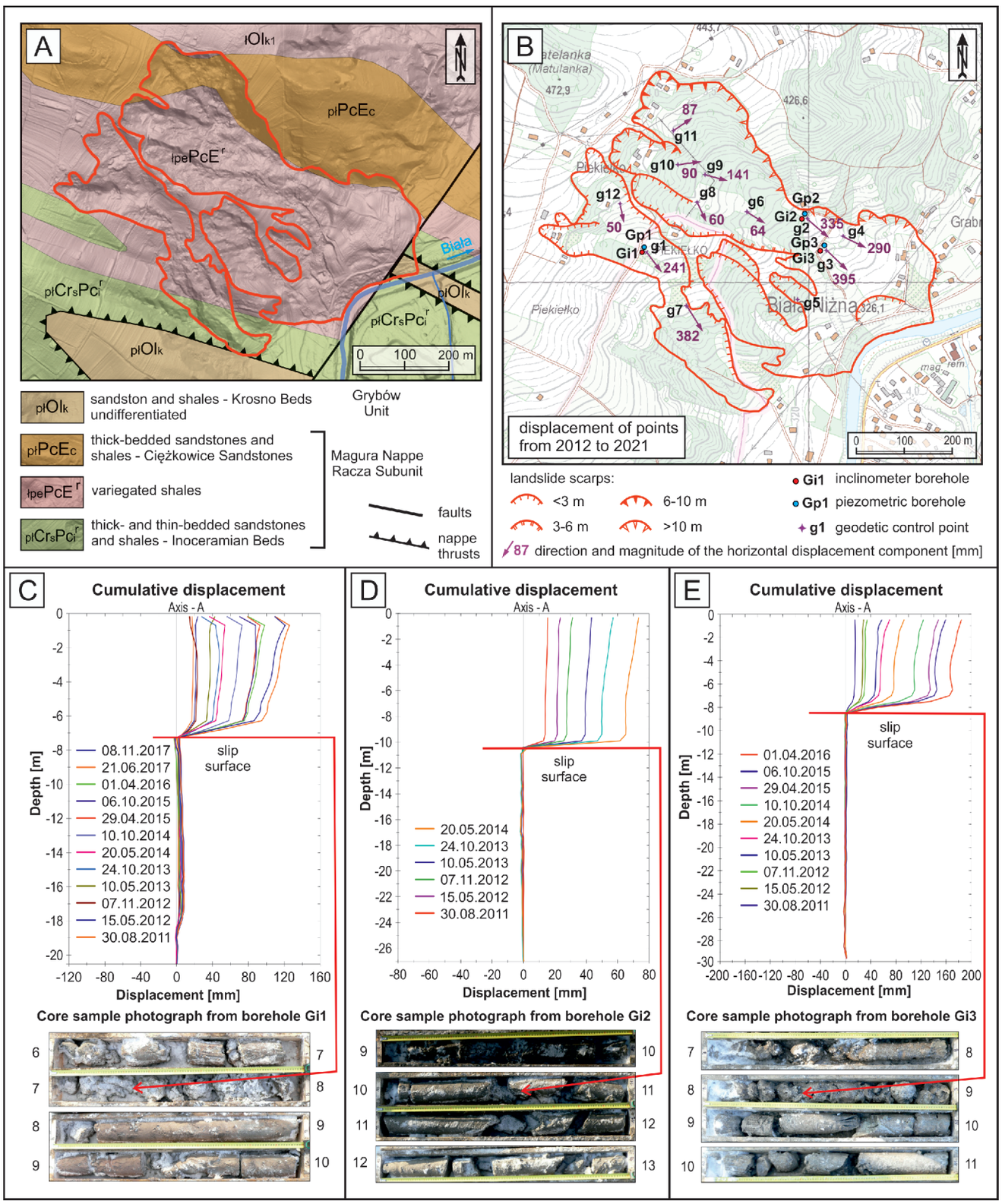

Fig. 4. The Grybów landslides

A – geological map superimposed on a DEM (after Paul, 1991); **B** – deployment of geodetic control points on the landslides; **C** – displacement graph for inclinometer Gi1 and core sample photograph; **D** – displacement graph for inclinometer Gi2 and core sample photograph; **E** – displacement graph for inclinometer Gi3 and core sample photograph

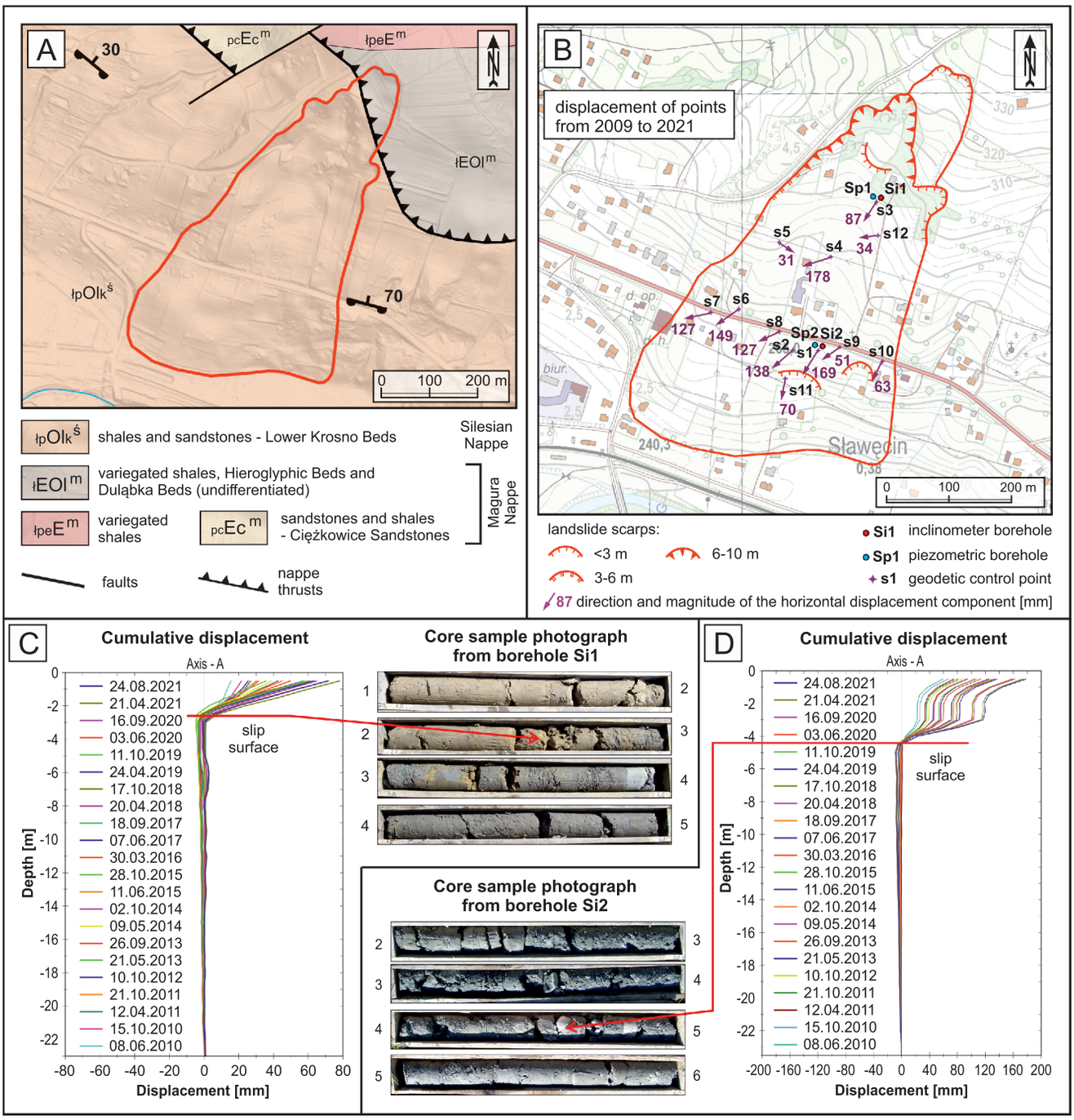

Fig. 5. Sławęcin landslide

A – geological map superimposed on a DEM (after Wójcik et al., 1992); **B** – deployment of geodetic control points on landslides; **C** – displacement graph for inclinometer Si1 and core sample photograph; **D** – displacement graph for inclinometer Si2 and core sample photograph

– surface monitoring relying mainly on geodetic methods;
– recording of rainfall and groundwater level fluctuations as factors that can activate landslides (Nescieruk and Rączkowski, 2012; Wojciechowski et al., 2012).

To characterize temporal changes in displacement rates, inclinometer measurements were used, whereas displacements of geodetic points installed on the landslides depicted the overall activity status. In addition, rainfall data from tipping-bucket gauges and groundwater-level variations from piezometers located on the landslides were recorded. Inclinometer profiling enabled precise tracking of the depths of deformation zones. Repeated surveys were conducted with a biaxial RST Digital Inclinometer, and displacements were computed using the Inclinalysis software (RST Instruments Ltd.). According to the instruments' technical specifications, the displacement measurement error is ±2 mm per 25 m.

Geodetic surveys enabled tracking of point trajectories in a planar Cartesian coordinate system. Twelve benchmarks were

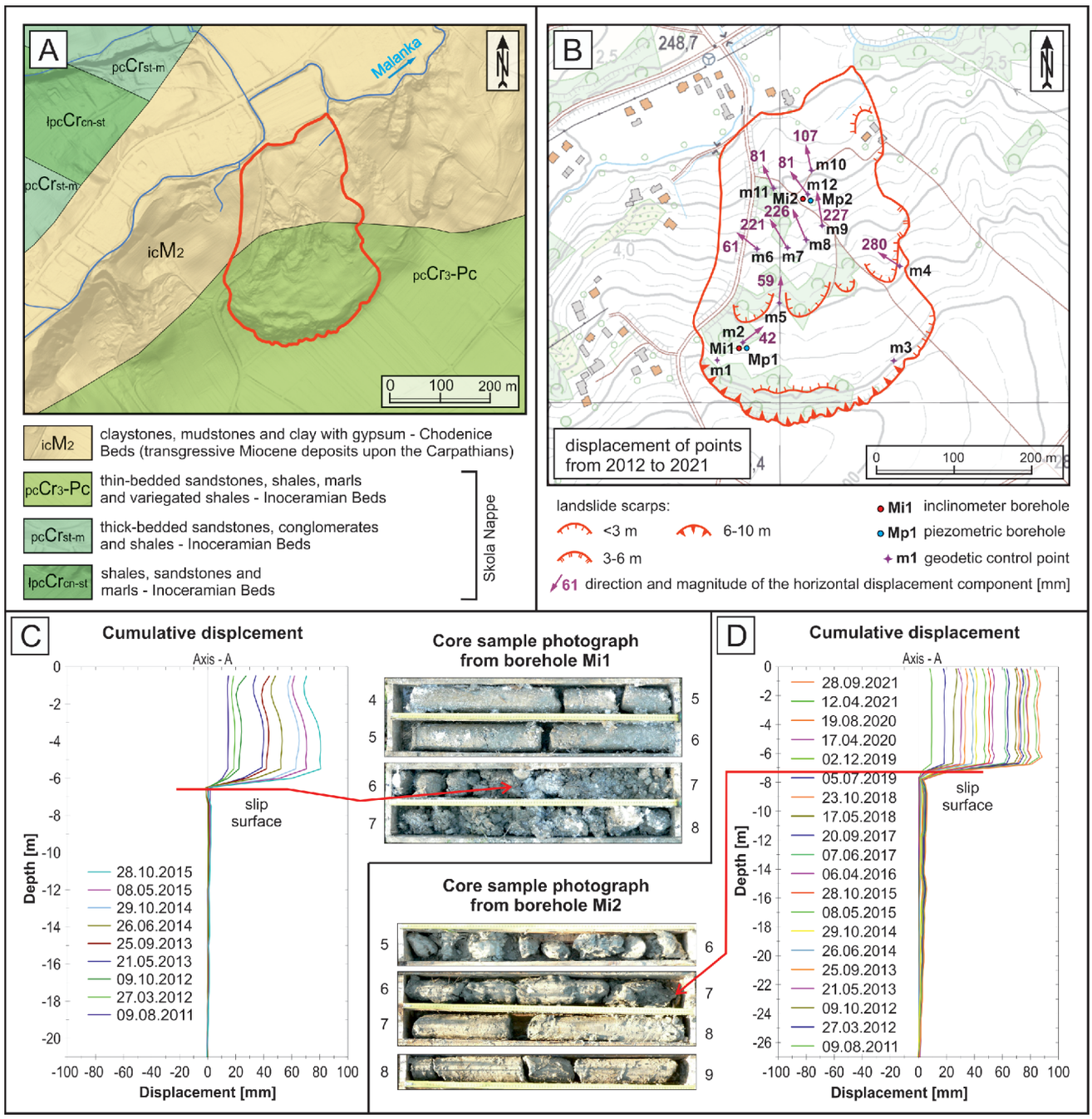

Fig. 6. Mała landslide

A – geological map superimposed on a DEM (after Szymakowska-Birkenmajer et al., 2014); **B** – deployment of geodetic control points on landslides; **C** – displacement graph for inclinometer Mi1 and core sample photograph; **D** – displacement graph for inclinometer Mi2 and core sample photograph

installed on each landslide. Benchmark positions were determined using Global Navigation Satellite (GNSS). Real-time kinematic measurements were conducted with ASG-EUPOS corrections. The initial surveys employed a Trimble R8 receiver, which, according to its specifications, provided horizontal accuracy of 30 mm and vertical accuracy of 50 mm in kinematic mode. The final surveys used an Emlid RS2 receiver, offering 10 mm horizontal and 15 mm vertical precision. For consistency, a simplified positional accuracy of ~30 mm was adopted, and, given slope inclinations below several tens of degrees, horizontal displacements subject to larger errors than the expected movements were not considered. Owing to this precision and the slow displacement rates, time series of point trajectories are not shown. The absence of detectable geodetic point movement indicates either landslide inactivity or displacements below the assumed error threshold.

Atmospheric precipitation was recorded using tipping-bucket rain gauges installed on the landslides. These instru-

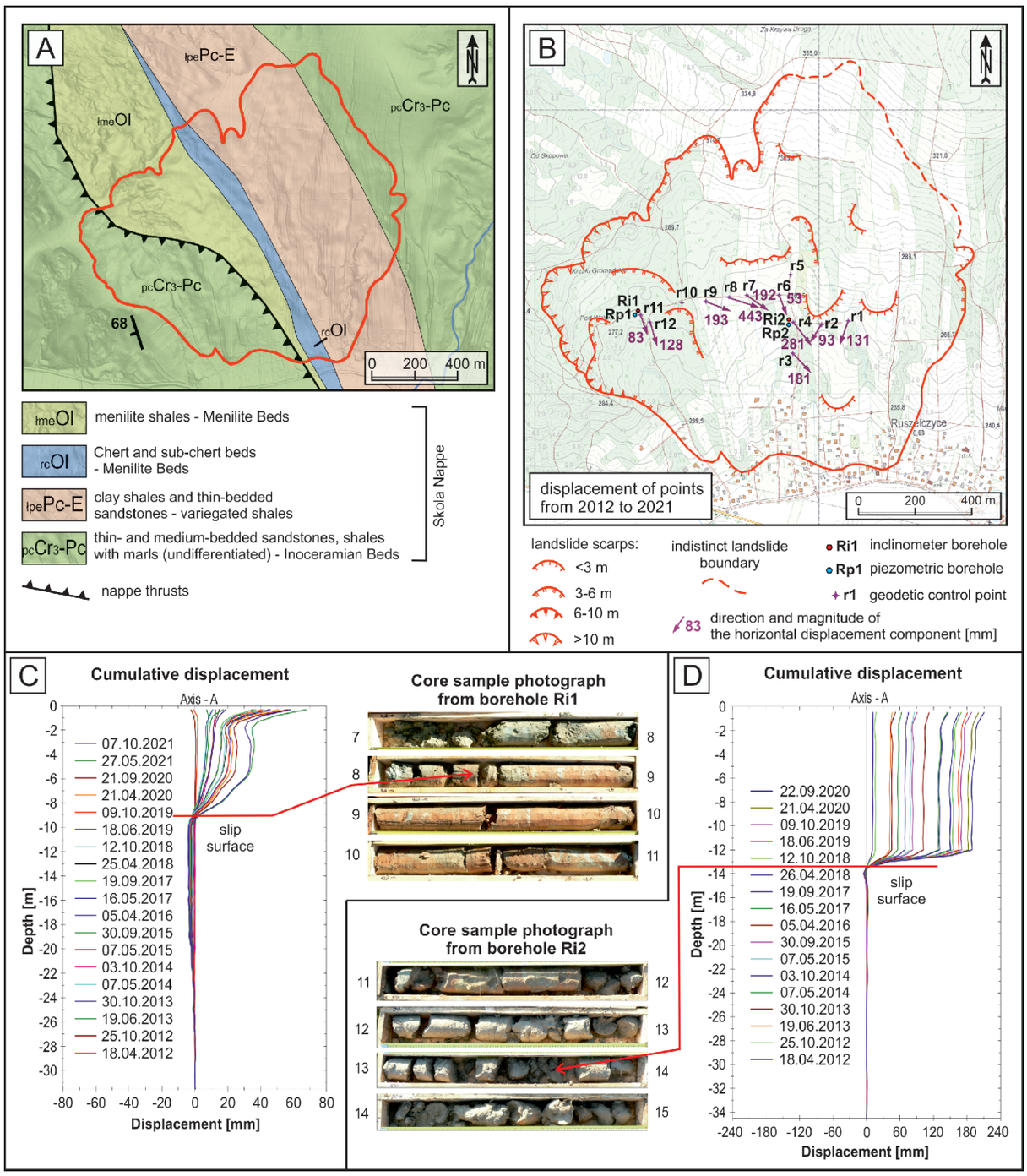

Fig. 7. Ruszelczyce landslide

A – geological map superimposed on a DEM (after Wasiluk and Gaździcka, 2018); **B** – deployment of geodetic control points on landslides; **C** – displacement graph for inclinometer Ri1 and core sample photograph; **D** – displacement graph for inclinometer Ri2 and core sample photograph

ments were unheated; consequently, winter precipitation was registered only during above-freezing air temperatures, assumed to approximately correspond to periods of snowmelt and, thus, to infiltration into the ground.

To track groundwater-level variations, automatic data loggers were installed in piezometer wells located adjacent to the inclinometer boreholes. Keller water-level recorders, model DCX-16, were installed on the landslides described. The total error band of these recorders is 0.1% of the full-scale range, which extends from 0 to 20 m of water column. In wells Gp1, Sp2, and Mp1, which were not equipped with loggers, the water table was measured using a manual electric water level meter on the same dates as the inclinometer surveys.

This article does not provide the results of laboratory tests conducted on rock samples. Selection and sampling of specimens for laboratory testing is a distinct and complex issue when aiming to obtain samples representative of landslide colluvium composed of fractured, weathered, and folded flysch. During

sampling, sections that are compact and approximately homogeneous are usually selected, namely near-surface clay layers or compact rock fragments. Parameters obtained from such material reflect the mechanical properties of the rock mass significantly different from those of the rock body forming the colluvium. Determining the position of slip surfaces during drilling is often problematic, particularly in fault-adjacent zones or thrust-overlap areas. These parameters should not be regarded as representative of colluvium. Establishing a credible association between these data and the analysis in the manuscript, and deriving valid conclusions, would be problematic.

RESULTS

GNSS AND INCLINOMETRIC MONITORING RESULTS

The monitoring results shown cover the period from the start of measurements to 2021. Some inclinometer casings were truncated earlier, therefore the monitoring intervals differ and are indicated by the measurement dates shown on the displacement graph for the inclinometers (Figs. 2C, D; 3C; 4C–E; 5C, D, 6C, D and 7C, D). The geodetic benchmark displacements reported on the landslides are based on the first and last GNSS measurements within that period (Figs. 2B–7B). Because this method has substantially lower precision, no detailed analysis of displacements using GNSS was performed later in the text as was done for the inclinometer measurements.

WITANOWICE LANDSLIDE

Geodetic monitoring commenced in March 2012. Twelve geodetic control points were installed in the upper and central sectors of the landslide (Fig. 2B); the lower sector was omitted due to dense vegetation. GNSS measurements revealed displacements exceeding the measurement error at 11 of the 12 points. The greatest movement was recorded at point w4 (377 mm), with slightly smaller values at w1 (265 mm), w3 (259 mm), w2 (258 mm), and w5 (221 mm). Displacements at the remaining points ranged from 157 to 38 mm.

Inclinometric monitoring on the Witanowice landslide since March 2012 detected deformation at two depths – 9.8 m and 26.6 m (Fig. 2C). After nearly four years, the inclinometer string sheared at the deeper slip surface, and subsequent measurements were therefore limited to 25 m depth. Over the next five years, shearing occurred at the shallower horizon of 9.8 m (Fig. 2D). Cumulative displacement profiles indicate a relatively narrow shear zone. The shallow slip surface lies within a decimetre-thick layer of plastic clays bounded above by soft, smoothly fissile shales and below by black clays containing sandstone fragments. The deeper slip surface follows the contact between clayey shales and a thin bed of dark green sandstone, where a ~0.4 m interval of crushed shale and slickensides was documented (Fig. 2C). Inclinometer results therefore classify this feature as a deep-seated landslide with listric slip surfaces.

ŻEGOCINA LANDSLIDE

Geodetic surveying at the Żegocina landslide was initiated in May 2012. For the first five years, measurements were confined to six control points (z1–z6), and in April 2017 an additional six points (z7–z12) were installed. The points are evenly distributed across the landslide except in the lower sector, where tall trees severely impede GNSS observations (Fig. 3B). Of the twelve points, seven showed displacements exceeding the measurement error. The greatest movement was recorded at point z5 (72 mm) in the central sector. Slightly smaller values were obtained at z10 (61 mm), z11 (59 mm), and z9 (57 mm), despite the measurement period for these points being only half as long, suggesting heightened activity in the lower portion of the slope. Point z4, which is mounted on the inclinometer casing, showed displacements comparable to those measured by the inclinometer string.

Inclinometric monitoring at Żegocina has been conducted since May 2012 in a borehole located in the central part of the landslide. The active slip surface was identified at a depth of ~11.5 m (Fig. 3C). Deformation of the inclinometer column occurred over a 1.5 m interval coinciding with a zone of crushed and slickensided sandstones. This indicates that displacements concentrate within a mechanically weakened horizon of the rock mass. Over nine years, cumulative displacements have reached ~35 mm.

GRYBÓW LANDSLIDES

Geodetic control points were installed primarily on the larger of the two landslides investigated in Grybów (Fig. 4B). The distribution of points across the landslide was constrained by areas of dense tree cover. GNSS surveys conducted from April 2012 through May 2021 revealed pronounced activity at all but one location, point g5, which lies at the slide's boundary. On the smaller landslide nearer the centre of Grybów, three control points were monitored: the greatest displacement occurred at g7 (382 mm), followed by g1 (241 mm) adjacent to inclinometer Gi1, and the least at g12 (50 mm). A similar pattern emerged on the larger landslide: significantly larger displacements were recorded at g3 (395 mm), g2 (335 mm), and g4 (290 mm) in the lower sector compared to the mid and upper parts.

Inclinometric monitoring in Grybów has been carried out since March 2011 across three boreholes. From the outset, each inclinometer casing recorded measurable deformation. Borehole Gi1 is located in the upper section of the smaller landslide, whereas Gi2 and Gi3 lie in the central section of the larger landslide (Fig. 4B). In Gi1, the active slip surface was identified at ~7.2 m below ground level (Fig. 4C), where the drilled core revealed crushed shale. Displacement increments were observed over a one-metre interval. The final reading before the inclinometer casing was immobilized was taken in November 2017, by which time cumulative displacement had reached 110 mm. The progressive tilting of the casing in the direction of movement indicates a predominantly translational mode of failure. In borehole Gi2, the slip surface occurs at a depth of 10.5 m below ground level (Fig. 4D). Core logs show that this horizon lies within a zone of gray, weak shales. The narrow, discrete shear zone caused rapid shearing of the inclinometer casing, and the last viable measurement was obtained in May 2014, with cumulative displacement amounting to only 65 mm. Due to a comparable rate of movement recorded in Gi3, monitoring in that borehole was continued over an extended period. In borehole Gi3, the slip surface was encountered at a depth of 8.3 m below ground level (Fig. 4E). The core revealed a 0.5 m thick horizon of weak shales. Monitoring in this hole ceased in April 2016, at which time cumulative displacements exceeded 170 mm over nearly five years.

SŁAWĘCIN LANDSLIDE

GNSS measurements on the Sławęcin landslide began in November 2009. Initially, ten control points (s1–s10) were monitored, and two additional points (s11 and s12) were installed in March 2017 (Fig. 5B). These points are mainly located along road no 28. During the road repair in 2019, points s7–s10 were destroyed, and point s5 was likely damaged by agricultural machinery. Consequently, displacement records for these points cover a shorter period, yet their magnitudes indicate movement rates similar to adjacent points. All twelve benchmarks showed displacement, with the maximum of 178 mm recorded at point s4 (Fig. 5B). GNSS data reveal slightly higher activity in the central sector of the landslide. Displacement magnitudes at points s1 and s3 – mounted on the casings of inclinometer boreholes Si1 and Si2 – are comparable to those measured within the inclinometer installations.

Inclinometric monitoring at Sławęcin has been conducted in two boreholes since November 2009, encompassing the catastrophic May 2010 rainfall event. Displacements during that interval are markedly greater than at other times. In borehole Si1, the active slip surface is located at 2.6 m below ground level (Fig. 5C). A distinct bend and downslope inclination of the inclinometer string indicate a translational mode of movement. Cumulative displacement at the upper end of the inclinometer column reached nearly 80 mm over the monitoring period. Core logs identify the slip surface as a thin (decimetre-scale) zone of plastic silts. In borehole Si2, the slip surface occurs at ~4.5 m depth (Fig. 5D). During the period analysed, measured displacements reached 120 mm above the slip horizon and 180 mm at the upper casing end. The core shows that the slip surface lies within crushed marly shales containing sandstone and siltstone fragments in a chaotic fabric.

MAŁA LANDSLIDE

Geodetic monitoring of the Mała landslide has been concentrated mainly in the central sector (Fig. 6B), where tree cover is absent. Measurements conducted from March 2012 to October 2021 revealed displacements exceeding the measurement error at 10 of the 12 benchmarks. The greatest movements were recorded at points m4 (280 mm), m9 (227 mm), m8 (226 mm) and m7 (221 mm). At the remaining points, displacements ranged from 42 mm to 102 mm. Points m1 and m3 were installed on the lower portion of the main scarp rather than within the colluvial apron, which likely explains why no movements were registered at these locations.

Inclinometric monitoring was carried out in two boreholes and indicated a constant displacement rate over the entire measurement period (Fig. 6C, D). In borehole Mi1, the slip surface was documented at a depth of 6.5 m below ground level (Fig. 6C). The last reading in October 2015 showed cumulative displacement of 73 mm. The upper section of the inclinometer casing tilted opposite to the slope's inclination, indicating a rotational failure mechanism. In borehole Mi2, the slip surface lies at 7 m below ground level within weak clays (Fig. 6D). Deformation occurred within a 1 m-thick zone, and maximum displacements of up to 90 mm were recorded during the monitoring period.

RUSZELCZYCE LANDSLIDE

GNSS monitoring of the Ruszelczyce landslide was conducted since December 2010. Control points were installed in the central sector of the landslide (Fig. 7B). The site includes numerous difficult-to-access areas densely covered by shrubs and fenced agricultural fields. Measurements at points r2, r4–r6, r8, r9, and r11 were carried out until October 2021, while for points r1, r3, r7, r10, and r12 the monitoring period is shorter. Canopy growth of trees and shrubs limited the precision of the GNSS observations. Displacements exceeding the measurement error were recorded at 10 of the 12 points, with the greatest movement measured at point r8 (443 mm). Point r4, mounted on inclinometer borehole Ri2, was displaced by 281 mm, whereas the inclinometer column recorded 210 mm over a period 2.5 years shorter. Velocities derived from both GNSS and inclinometry are comparable. Point r11, installed on borehole Ri1, moved 83 mm, matching the inclinometer readings.

Inclinometric measurements in the central sector (Fig. 7B) reveal distinct activity zones. In borehole Ri1, the slip surface appears at ~8.5 m below ground level (Fig. 7C). Above this horizon, the inclinometer string tilts downslope, indicating translational movement. Over ten years, cumulative displacement in the Ri1 column reached nearly 70 mm. In borehole Ri2, the active slip surface lies at ~13.6 m depth (Fig. 7D). Weak clays occur both above and below this surface, which likely permitted displacement measurements reaching nearly 200 mm.

RELATIONS BETWEEN DEFORMATIONS, RAINFALL AND GROUND WATER

The main element of analysis of the landslides investigated involved correlating precipitation data with variations in subsurface water levels and incremental displacements recorded in inclinometer casings. The determination of the timing of activity changes was reduced to identifying the most adverse meteorological conditions that precipitate a pronounced alteration of the hydrogeological regime. For this, a detailed examination was conducted for each landslide over selected time intervals, during which the impact of rainfall on groundwater levels was assessed and an attempt was made to pinpoint the specific precipitation event that triggered changes in landslide velocity.

WITANOWICE LANDSLIDE

Inclinometric monitoring from the outset demonstrated that the landslide is active (Fig. 8). Two slip surfaces were identified at depths of 9.8 m and 26.6 m b.g.l. The more rapid shearing of the deeper horizon is attributed to its narrow shear zone.

Two distinct time intervals exhibiting increased displacement rates were analysed in detail (Fig. 8). The first interval, between inclinometer surveys on 9 April and 19 September 2014, spans the wet spring and summer months, during which several high-intensity rainfall events occurred. Cumulative displacements increased by 13 mm on the deeper slip surface and by 6 mm on the shallower surface. The surge in activity likely began in mid-May following heavy rainfall. A similar increment was recorded in the June 2015 survey, despite relatively low monthly rainfall at that time. The second interval covers 31 May to 30 November 2017. After a relatively dry June 2017, rainfall rose through July and August, peaking at 194 mm in September, then declined toward the end of the period. Inclinometer measurements during this interval were limited to a shortened column. No displacements were recorded between the 31 May and 27 September 2017 readings. The most substantial rainfall in late September 2017 coincided with a piezometric water-level rise of over 1 m, likely triggering landslide reactivation. Displacements between 27 September 2017 and 30 April 2018

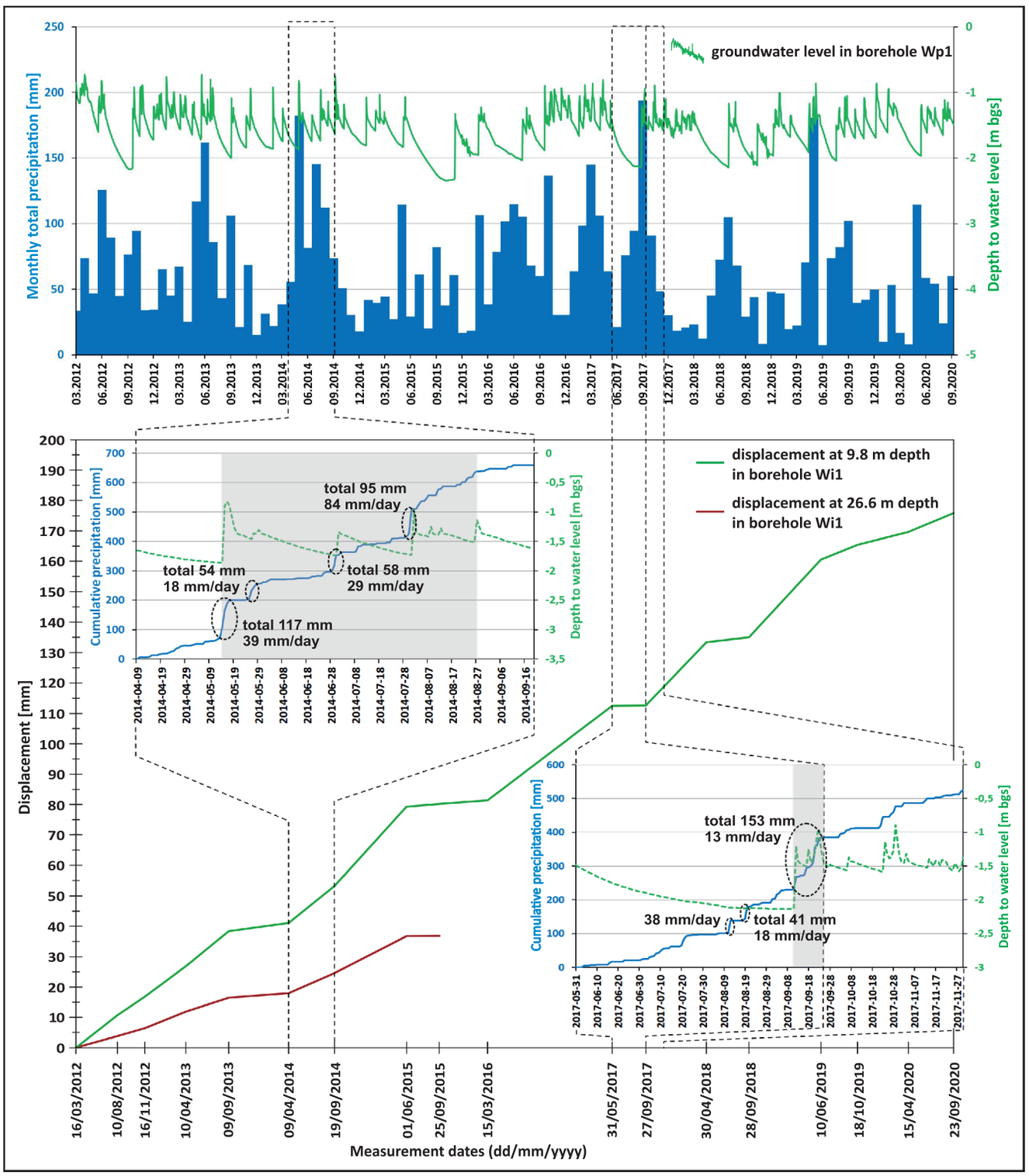

Fig. 8. Temporal comparison of precipitation, groundwater level variations, and ground displacements within the Witanowice landslide

amounted to 21 mm. Considering the timing of the water-level rise, the landslide's response to precipitation showed a lag of at least two weeks. By analogy, the first interval's acceleration probably commenced between May and June 2014.

ŻEGOCINA LANDSLIDE

Inclinometric monitoring over a 9-year and 4-month period recorded cumulative displacements of 33 mm. Landslide activity fluctuated during this interval: the bulk of movement occurred

between September 2012 and May 2014 and again between June 2018 and October 2019, while only minor activity was noted from February 2016 to September 2017 and from April to September 2020 (Fig. 9).

Three distinct intervals of accelerated movement were selected for detailed analysis. The first and third intervals include several preceding weeks to capture major rainfall events. Between 27 June and 13 November 2013, relatively large deformation events were observed (Fig. 9). June 2013 was exceptionally wet, with a total of 331 mm of precipitation. Rainfall of 95 mm from 3–5 June induced a rapid piezometric water-level rise of 5 m, and a further 104 mm fell on 11–12 June. Additional storms in late June and mid-July produced further pronounced water-level increases. The final rise in this interval occurred between 2 and 9 November, indicating that the landslide acceleration could have begun any time between 3 June and 18 July; displacements may also have occurred between 9 and 11 November 2013. During the second interval, between inclinometer readings of 12 June and 20 September 2018, total movement amounted to 2 mm (Fig. 9). The piezometric level remained near 10 m below ground until a small (<1 m) rise followed late-June rains, but a substantial rise from 10.2 to 5.8 m b.g.l. resulted from 293 mm of rainfall between 16 and 19 July. The recorded displacement correlates with this intense precipitation. The third interval mirrors the first in its meteorological pattern: successive multi-day heavy rains from 27 April to 24 May 2019. The most adverse conditions – producing marked piezometric changes – occurred two to six weeks before the inclinometer survey on 11 June 2019. This timing suggests movement initiation in May, continued velocity increase after 11 June, and subsequent deceleration. Earlier displacements measured between September 2018 and June 2019 likely stem from the May 2019 rainfall.

GRYBÓW LANDSLIDES

Greater displacements were initially recorded in borehole Gi1 on the Grybów landslides. Over the first five months they totalled 18 mm, whereas during the subsequent fourteen months they amounted to only 5 mm. Borehole Gi2 showed an approximately constant displacement rate of about 1.8 mm/month. This installation sheared after 38 months, by which time cumulative displacement had reached 67 mm. The largest movements were observed in borehole Gi3, where displacements over a five-year period totalled 173 mm, corresponding to an average rate of 2.9 mm /month.

Two distinct time intervals showing accelerated displacement were analysed in detail for the Grybów landslides (Fig. 10). The first interval spans the inclinometer surveys of November 2012 and May 2013, while the second extends from 1 April to 10 October 2014. The latter interval was back dated to encompass the exceptionally heavy rainfall of April–May 2014. In the first interval, all three inclinometer casings recorded comparable displacement magnitudes, and no significant influence of rainfall on piezometric water-level fluctuations was detected. From January through early February, nearly continuous but low-intensity precipitation occurred at an average rate of 2.5 mm/day. Between 11 March and 13 April total rainfall amounted to 106 mm, comprising short, intense events in March and less intense yet prolonged rains in April. It remains uncertain which specific rainfall pattern most strongly governed the observed increase in displacement rates. During the second interval, increased displacements were observed in boreholes Gi1 and Gi3, and the inclinometer in Gi2 sheared following the 20 May 2014 reading. Monthly precipitation totals were 211 mm in May, 236 mm in July, and 160 mm in August. A particularly intense event on 14–17 May delivered 148 mm of rain, inducing a piezometric rise of over 2 m in P3 and likely initiating the landslide's acceleration phase. Additional heavy rainfall from 9 to 12 July, followed by moderate but regular precipitation through late July and August, sustained high water levels in P3 throughout the interval. The water level in P1 – monitored from mid-July after instrument repair – remained stable at ~4.5 m b.g.l. Dip-tape readings in P2 during May and October indicated slightly shallower levels than those recorded in most other measurements. Assuming the acceleration after 20 May was triggered by the mid-May storm (14–17 May), the lag time between peak rainfall and landslide response is estimated at a minimum of three days.

SŁAWĘCIN LANDSLIDE

Inclinometric baseline monitoring on the Sławęcin landslide was conducted in November 2009, with the next survey carried out three weeks after the catastrophic spring 2010 rainfall. Measurements on 8 June 2010 recorded displacements of 17 mm in inclinometer casing Si1 and 24 mm in casing Si2 (Fig. 11). Over a 12-year period, cumulative movements reached ~65 mm in Si1 and nearly 130 mm in Si2. In Si2, the impact of intense precipitation during May–June 2014 and July 2019 is clearly reflected in accelerated landslide activity. Periods of relative stability coincided with intervals of low rainfall, and incremental displacements in Si2 were generally larger in spring surveys than in those conducted in autumn.

Three distinct time intervals marked by elevated landslide activity coinciding with peak monthly rainfall totals were selected for detailed analysis (Fig. 11). The discussion focuses on inclinometer casing Si1, since alternating increments and reductions in displacement within casing Si2 impede a consistent interpretation of activity. This behaviour in Si2 likely reflects episodic loading of the probe by earth masses and the casing's response within weak substrate. During the first interval, manual groundwater measurements in piezometer Sp1 indicated shallow ponding at ~0.5 m below ground level (b.g.l.), while Sp2 showed no significant water-level change despite heavy May–June 2010 rainfall. Total rainfall in May 2010 reached 254 mm, with 130 mm falling between 15–16 May and a further 122 mm from 30 May to 4 June. The concurrent surge in landslide displacement is attributed to these heavy rainfall events. The second interval spans 9 May to 2 October 2014, during which casing Si2 accumulated 8 mm of displacement. Heavy rainfall occurred in mid-May, late June, and early July 2014; piezometer Sp1 recorded a 0.5 m water-level rise, whereas Sp2 remained essentially constant. Rainfall totals included 89 mm between 11–17 May, but the larger pulses of 56 mm in late June and 129 mm in early July more plausibly drove the observed acceleration. A subsequent stabilization recorded in Si2 during September likely reflects the dry conditions of that month. The third interval, bounded by inclinometer readings on 24 April and 11 October 2019, saw casing Si2 displace 17 mm, while Si1 showed occasional downslope reversals, a pattern observed throughout the monitoring period. May 2019 was the wettest month on record with 233 mm of rain – half of which fell over a three-day span – correlating with the first phase of landslide acceleration. A secondary uptick in activity may also link to 121 mm of rainfall in the first half of August. At the start of this interval, Sp1's water table lay at 0.5 m b.g.l., rising to 1.4 m b.g.l. by October; Sp2 remained virtually unchanged. Although the

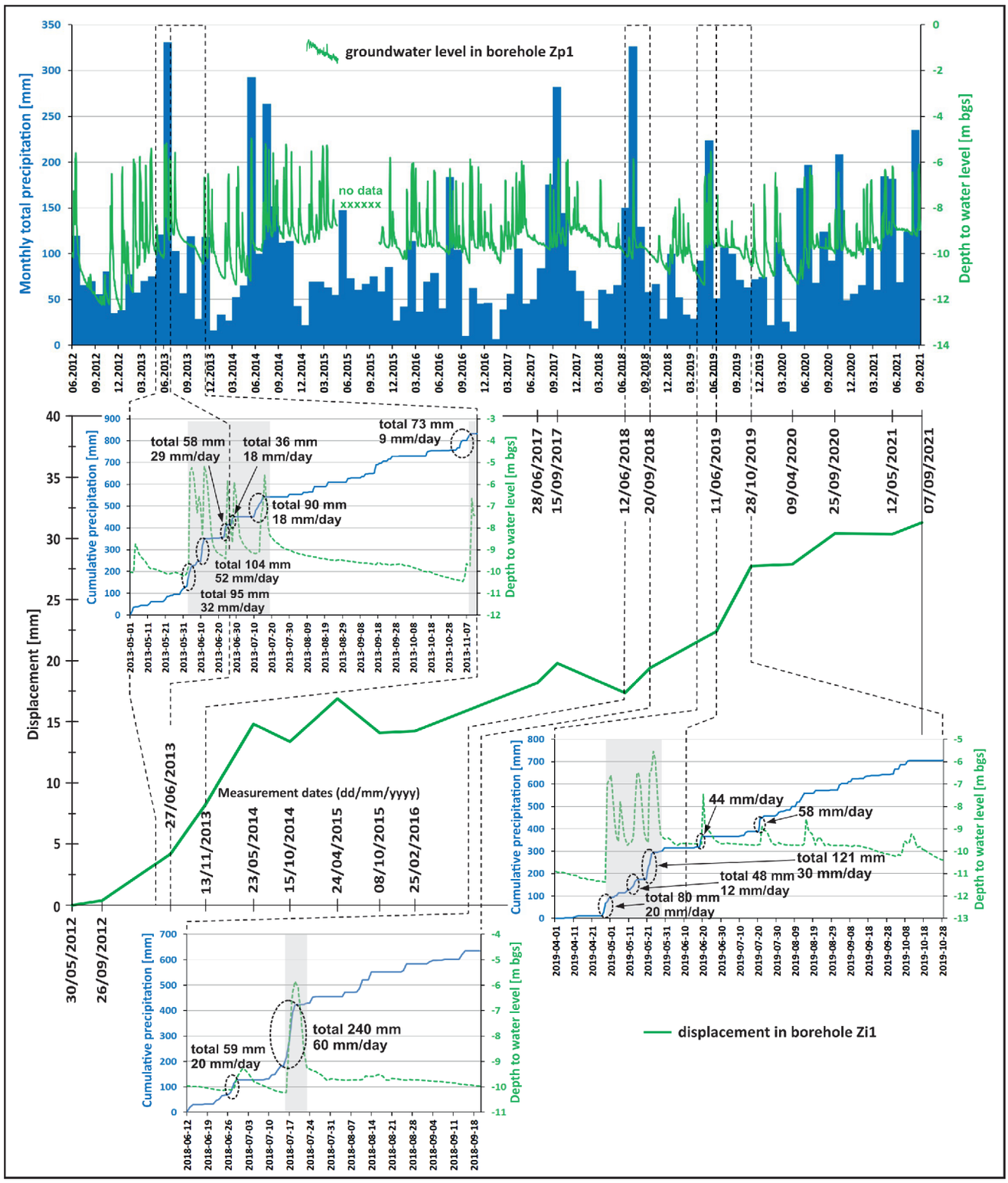

Fig. 9. Temporal comparison of precipitation, groundwater level variations, and ground displacements within the Żegocina landslide

piezometric levels showed limited response, the heavy rainfall events evidently exerted a significant influence on landslide dynamics.

MAŁA LANDSLIDE

The Mała landslide maintains a more consistent displacement rate than the other case studies described. In inclinometer

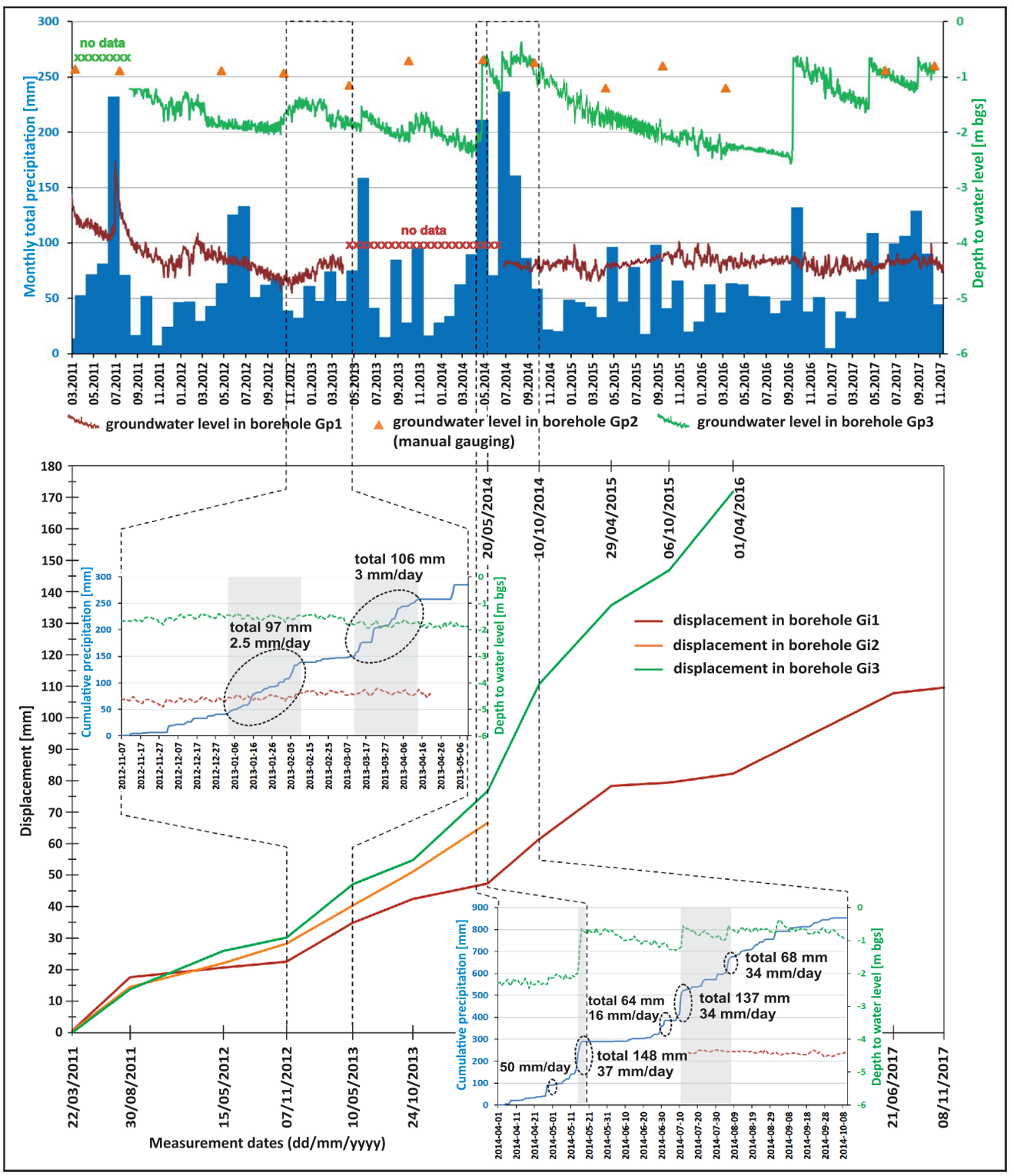

Fig. 10. Temporal comparison of precipitation, groundwater level variations, and ground displacements within the Grybów landslides

casing Mi1 the mean rate is 1.3 mm/month, whereas in Mi2 it is 0.7 mm/month. To evaluate the influence of precipitation on this landslide's activity, two discrete time intervals were analysed. The first spans the surveys of May and September 2013, during which Mi1 recorded a slight deceleration and Mi2 a pronounced acceleration. The second extends from 1 May to 29 October 2014, over which Mi1 exhibited a marked increase in velocity and Mi2 a modest rise.

The first interval began with two weeks of moderate rainfall averaging 6.5 mm/day, raising the water table in piezometer

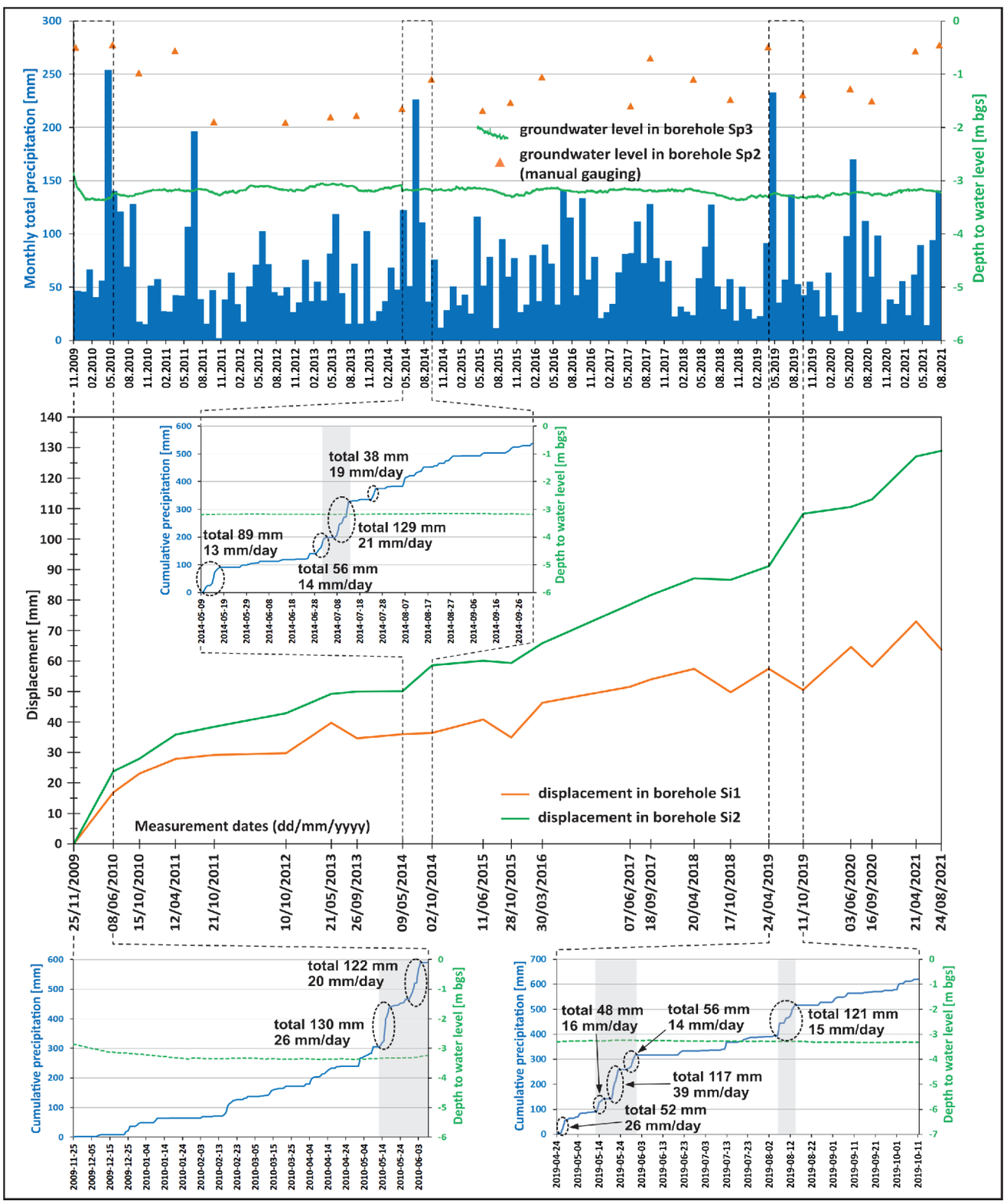

Fig. 11. Temporal comparison of precipitation, groundwater level variations, and ground displacements within the Sławęcin landslide

Mp2 by ~0.5 m. This period culminated in an intense storm on 10–11 June (44 mm), which likely triggered the activity spike in Mi2. Subsequent downpours on 23–24 June (74 mm) may have temporarily weakened slope stability. The observed slowdown in Mi1 during these heavy rains is difficult to explain, since Mi1's greatest movements occurred in other intervals with relatively low monthly precipitation. It is hypothesized that the upper colluvial layers impose a slowly varying load on the lower slope,

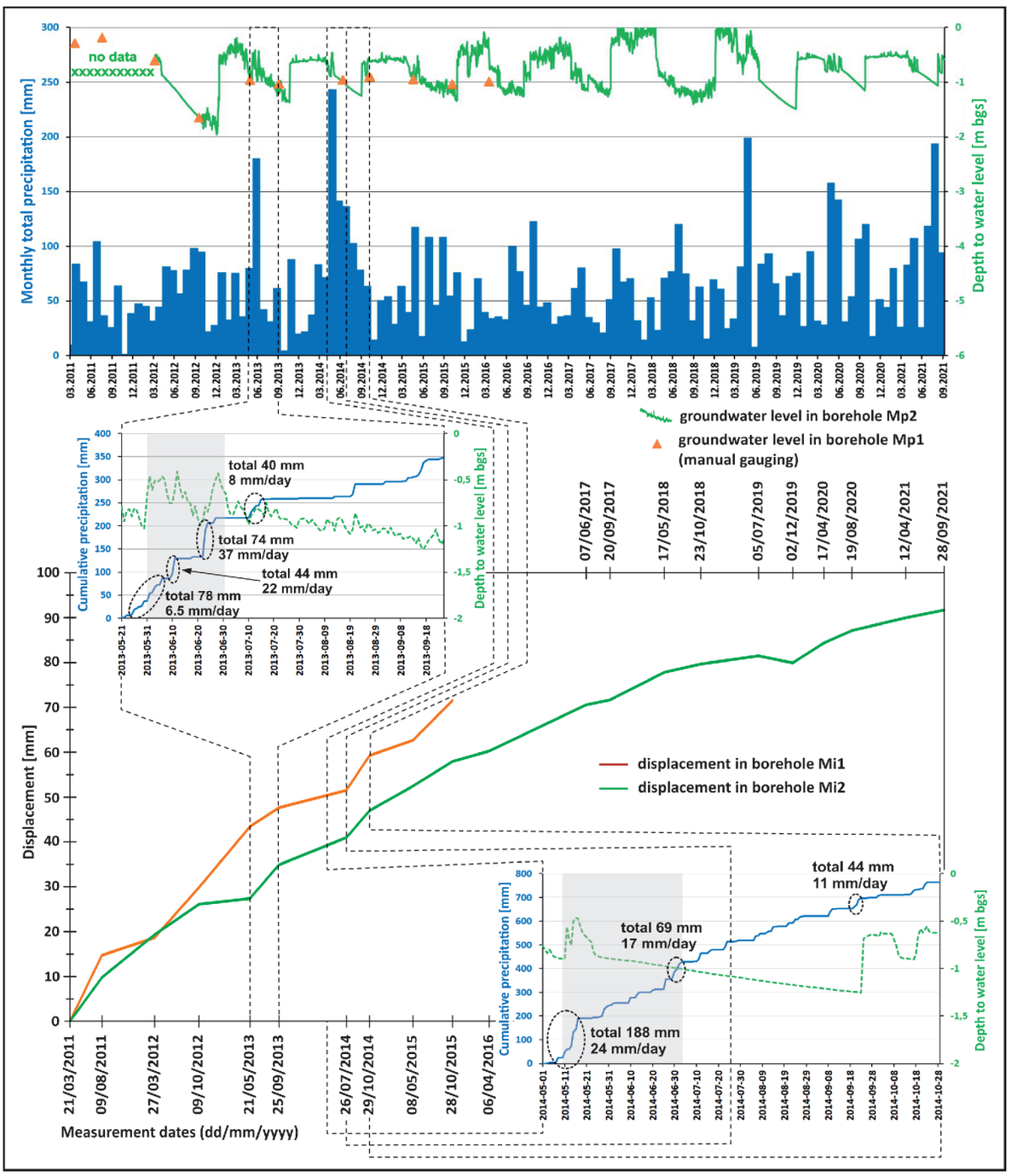

Fig. 12. Temporal comparison of precipitation, groundwater level variations, and ground displacements within the Mała landslide

causing a delayed, out-of-phase response between the two inclinometer casings and a lag relative to rainfall events. The second interval corresponds to the wettest season recorded over the entire monitoring period. After the 26 July 2014 readings, both Mi1 and Mi2 showed clear acceleration. May 2014 alone produced 243 mm of rain, after which monthly totals declined. In mid-May a multiday storm delivered 166 mm, lifting the piezometric level in P2 by ~0.5 m. In June and July, over half the days saw rainfall, with several events reaching as much as 43 mm/day. Notably, the landslide accelerated after 26 July 2014 despite lower totals of 102 mm in August, 78 mm in September, and 63 mm in October. This pattern indicates that the intense May storms, compounded by prolonged moderate precipitation, gradually but systematically undermined slope stability and drove the observed increase in displacement rate.

RUSZELCZYCE LANDSLIDE

Monitoring results indicate that the western sector of the Ruszelczyce landslide shows markedly lower activity than its central sector (Fig. 13). Cumulative displacement in inclinome-

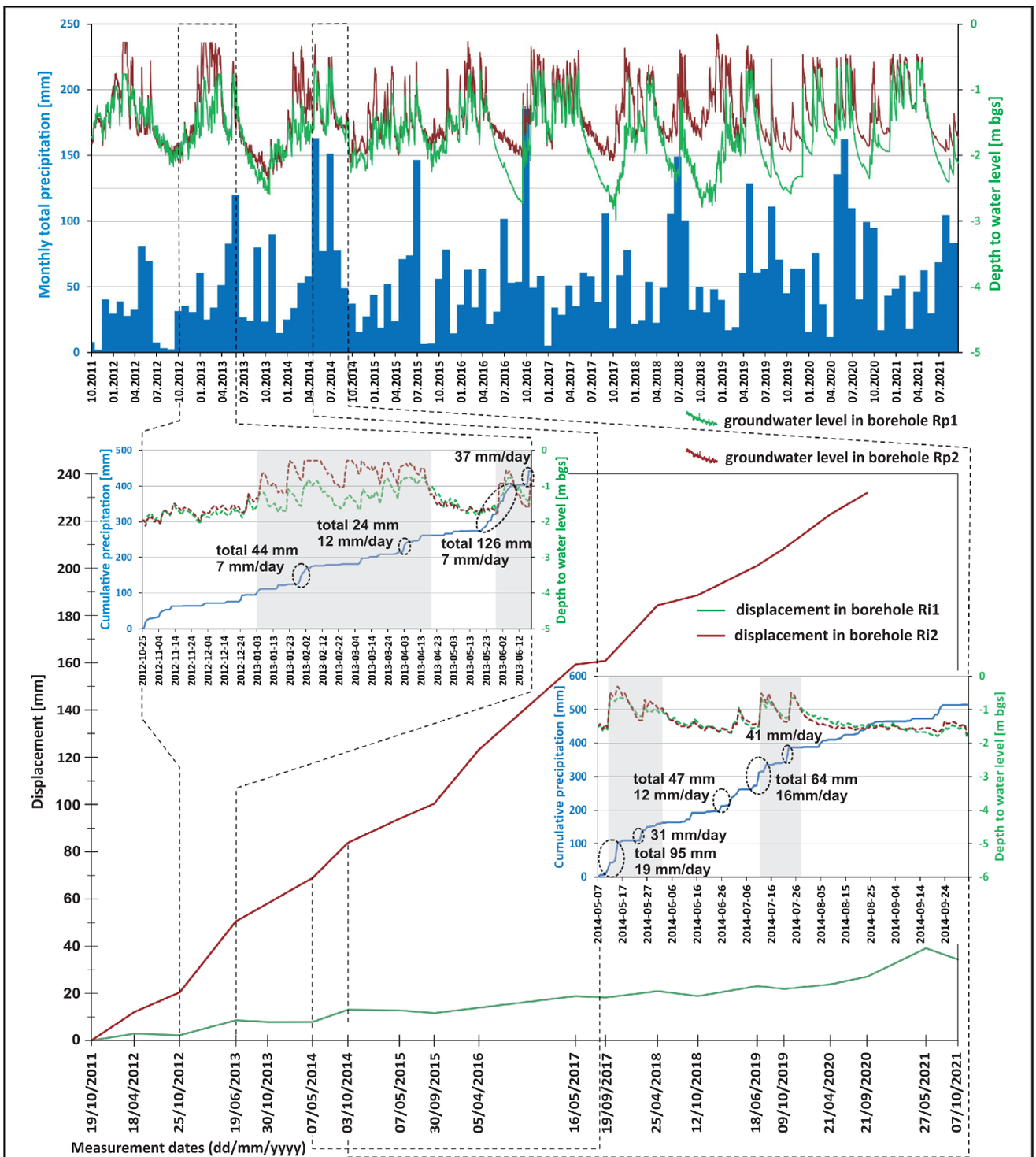

Fig. 13. Temporal comparison of precipitation, groundwater level variations, and ground displacements within the Ruszelczyce landslide

ter casing Ri1 reached 35 mm, whereas Ri2 recorded 232 mm. The highest activity occurred between October 2012 and June 2013; this interval is examined in detail below. A second interval, from 7 May to 3 October 2014, was also characterized, as both inclinometer columns showed a pronounced acceleration during this period.

The first interval was not exceptionally wet within the context of the entire monitoring record. Monthly precipitation ranged from a low of 25 mm in February 2013 to 120 mm in June 2013. Initially, piezometric levels in both boreholes lay between 1.5 and 2.0 m below ground level, rising by several tens of centimetres between January and April 2013. Short-term water-level fluctuations correlate with rainfall, and the February–March rise

likely reflects concurrent snowmelt. The combination of rainfall and snowmelt may have driven an uptick in landslide activity. Of particular significance are the May–June 2013 rains: 126 mm over 18 days induced a rapid piezometric rise of about 1 m in both instruments. This hydrological loading likely intensified landslide movement, especially given the slide's gentle (~5°), undulating surface, which hinders surface runoff and enhances infiltration. The second interval encompassed heavy precipitation in May and July 2014—intervals that also coincided with heightened activity at the other sites studied. Mid-May storms delivered 95 mm of rain over five days, lifting water levels by roughly 1 m and maintaining them for two weeks; these events likely triggered the landslide's acceleration. Subsequent moderate but persistent rains, including several intense showers in late June and July, produced further piezometric rises. Although July rainfall was less intense than in May, its extended duration continued to degrade slope stability and sustain elevated landslide activity.

DISCUSSION

The state of activity of all the landslides monitored is summarized in a single diagram (Fig. 14), which plots cumulative displacements recorded in every inclinometer casing on a common time axis. On that same time axis, monthly precipitation totals are shown, including the minimum, maximum, and mean values across all six study sites.

The precipitation plot reveals that the highest rainfall occurs predominantly in summer, with large disparities between minimum and maximum monthly amounts. During the monitoring period, the greatest monthly total – 331 mm – was recorded in June 2013 at the Żegocin gauge, while the mean for that month across all six sites was 178 mm. Notably high average rainfall also occurred in July 2011; May and July 2014; September 2017; July 2018; and May 2019 – intervals that coincided with surges in landslide activity (Fig. 14).

Displacement histories demonstrate near-continuous movement, with velocity fluctuations broadly tracking precipitation intensity. The fastest rate was recorded in casing Gi3 at Grybów, which showed an approximately constant velocity of 2.8 mm/month. According to Cruden and Varnes's (1996) classification, all of the landslides described here fall into the "very slow" to "slow" categories.

The cumulative displacement at which inclinometer casings sheared varied from 38 mm in casing Wi2 to 232 mm in casing Ri2. This range largely reflects differences in shear-zone thickness and the plasticity of the rock mass within those zones.

Over longer intervals, GNSS surveys provided an overview of whole-landslide activity, and benchmarks installed on inclinometer casings served to validate displacement magnitudes. Direct comparison of geodetic and inclinometric measurements over short (multi-monthly) intervals is precluded by their differing accuracies; however, over longer periods the methods effectively reference each another.

The landslides described here exhibited continuous activity, with varying displacement magnitudes over successive measurement intervals. Accelerations in movement typically coincided with prolonged periods of heavy rainfall, yet identifying a clear rainfall threshold and pinpointing the exact onset of acceleration is difficult. This challenge i salso expressed by Zabuski (2004), who characterized similar landslides under comparable geological settings as "quasi-continuous," in which movement proceeds slowly, may intermittently cease, but never becomes abrupt. In such contexts, more frequent monitoring would improve the resolution of the relationship between precipitation and displacement rate. Current detection of slow-moving landslides often relies on time-series analyses of InSAR imagery. Hu et al. (2016) observed a seasonal pattern of displacements in the Cascade landslide complex of Washington State that correlated with winter precipitation, and Handwerger et al. (2013) conducted analogous studies for landslides in northern California. These investigations further linked observed deformations to a one-dimensional linear diffusion model, estimating a landslide response time of ~40 days following the onset of seasonal rainfall. However, in the flysch-dominated Carpathians – where precipitation is highly variable – such analytical frameworks are unlikely to yield satisfactory results for slow-moving landslides. The complex hydrogeological structure of the flysch further complicates reliable modelling of landslide response to rainfall.

Several studies analysing landslide events in the Carpathians have established rainfall thresholds beyond which landslide activity intensifies. Gil (1997) estimated that, in flysch units dominated by sandstones, reactivation occurs after 400–550 mm of cumulative rainfall over 20–45 days, including a 5–6 day episode of intense downpours totalling 250 mm. In a later study, Gil and Długosz (2006) proposed a 500 mm threshold for prolonged, diffusive rain that triggers catastrophic landslide initiation – rainfall magnitudes that are exceptionally rare in the Carpathians. For slopes underlain by interbedded sandstones and shales, these authors reported lower thresholds of 250–300 mm over 20–45 days. Rączkowski and Mrozek (2002) further showed that structural landslides activate under either diffuse rain exceeding 400 mm, monthly totals above 600 mm, or convective storms delivering more than 250 mm. The high-precision monitoring results described here indicate that the actual precipitation amounts required to reactivate these slides are lower than previously reported, while the duration of exposure to rainfall emerges as the critical factor. In low-permeability bedrock, much of the intense rain runs off the slope surface without altering the physicomechanical properties of the colluvium. Consequently, long-duration rainfall – even at moderate intensities – plays a key role in reducing slope stability and precipitating renewed movement.

Landslides developed in flysch bedrock dominated by clayey units exist in a state close to the threshold of stability. These slides remain in continuous movement or accelerate during rainy periods when monthly precipitation approaches 100 mm (for example, the Grybów, Mała, and Ruszelczyce landslides).

This analysis indicates that in areas underlain predominantly by claystones, where infiltration of rainfall is impeded, the response time of landslides to precipitation is relatively long. The phases of acceleration and deceleration likewise extend over protracted intervals. Consequently, these landslides display an approximately steady level of activity that is difficult to correlate with variable rainfall patterns.

The Grybów landslides were among those studied by Perski and Wojciechowski (2022), who analysed InSAR observations from a reflector installed near inclinometer Gi1 and piezometer Gp1. Their results demonstrate minor reflector displacements at an average rate of ~20 mm/yr. They corroborated that modest fluctuations in groundwater level influence the deformation rate measured by radar reflectors. Seasonal oscillations in groundwater level were mirrored by sinusoidal variations in reflector displacement rate, albeit with a lag of approximately four months. These authors noted that the strength of this correlation depends on the local geological structure and that the precise response time remains difficult to define.

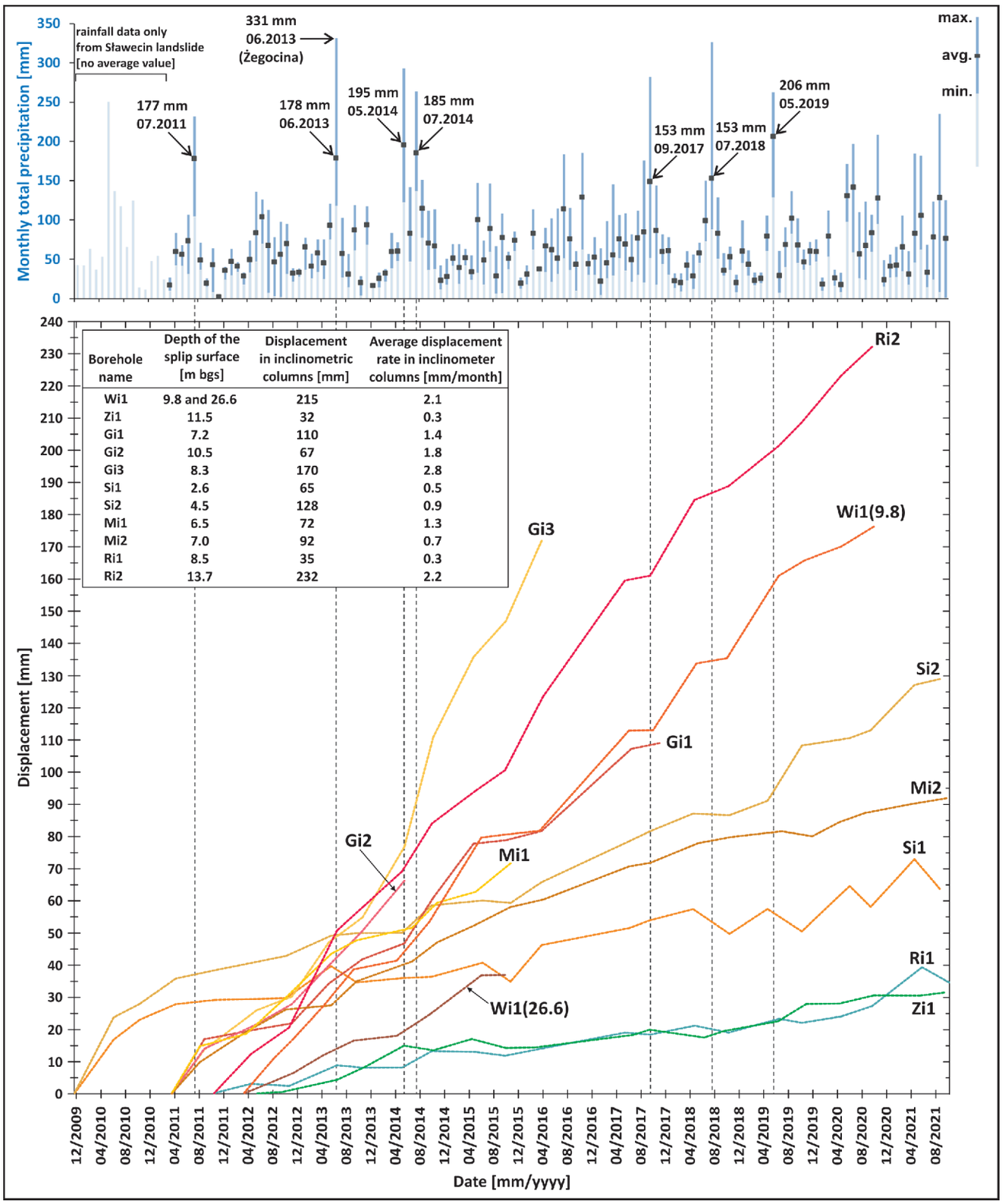

Borehole name	Depth of the splip surface [m bgs]	Displacement in inclinometric columns [mm]	Average displacement rate in inclinometer columns [mm/month]
Wi1	9.8 and 26.6	215	2.1
Zi1	11.5	32	0.3
Gi1	7.2	110	1.4
Gi2	10.5	67	1.8
Gi3	8.3	170	2.8
Si1	2.6	65	0.5
Si2	4.5	128	0.9
Mi1	6.5	72	1.3
Mi2	7.0	92	0.7
Ri1	8.5	35	0.3
Ri2	13.7	232	2.2

Fig. 14. Aggregate comparison of displacements recorded in inclinometer columns in relation to monthly precipitation totals at the landslides analysed

An important issue that warrants brief discussion is the general relationship between landslide activity, the bedrock on which the landslides developed, and the composition of the colluvium derived from those bedrock lithologies. The permeability of the parent rock appears especially significant. In areas where colluvium consists predominantly of clayey deposits, pore-water pressure, effective stress, and the consistency of deeper soil layers remain approximately constant and are only weakly dependent on short-term, fluctuating precipitation. These parameters change when precipitation remains steady over prolonged periods or during extended drought, whereas a rapid response to individual rainfall events can be associated only with substantial water loading of those landslides that are already oscillating near the stability threshold. A shallow and narrowly fluctuating water level measured in piezometers is, in my view, a poor indicator of changes in landslide activity.

CONCLUSIONS

This study indicates that landslides occurring in flysch rocks dominated by clay-rich deposits are in a state close to the stability threshold. These landslides remain in continual movement or accelerate during rainy periods when monthly precipitation totals approach 100 mm (e.g., the landslides at Grybów, Mała and Ruszelczyce). In low-permeability rocks a large portion of intense rainfall runs off the slope without altering the physico-mechanical properties of the colluvium. Consequently, prolonged precipitation, not necessarily of high intensity, is of key importance.

Analyses show that in areas underlain predominantly by clayey rocks, where infiltration of meteoric water is impeded, the landslide response time to rainfall is relatively long. The processes of landslide acceleration and deceleration are likewise distributed over a longer time span. Such landslides show approximately constant activity that is difficult to correlate with short-term, fluctuating precipitation.

This long-term monitoring supports recommendations for optimizing measurement frequency. For landslides exhibiting no field-observed motion and causing no persistent damage to engineering structures, biannual geodetic surveys appear sufficient. Such surveys are best conducted after signs of damage to buildings, roads, or utilities, when displacements are likely large enough to be detected by low-cost, widely applicable geodetic techniques.

Inclinometry reveals much smaller displacements than geodetic methods; therefore, for landslides of uncertain activity it is reasonable to perform inclinometer readings every two to three months initially. The first few measurements should guide any subsequent adjustment in frequency. Additional surveys are warranted during prolonged or intense rainfall (e.g., multi-day totals exceeding 100 mm) and during snowmelt accompanied by rain.

For landslides expected to move several centimetres per month, the cost and effort of installing inclinometer casings – and their limited functional lifespan – should be weighed against the expected benefit. Inclinometer data are most justified where precise knowledge of displacement rate and deformation-zone depth is critical for geotechnical slope-stabilization design.

Groundwater-level monitoring is principally warranted on landslides underlain by permeable or highly fractured rocks. In these cases, rainfall-induced water-table fluctuations can help establish precipitation thresholds and inform early-warning procedures. On clay-rich landslides – such as those described here – where activity is continuous and poorly correlated with rainfall, deformation monitoring is of greater importance.

Finally, in low-permeability strata, shallow perched water often shows rapid surface inflows followed by stagnation. Inclinometer boreholes on active landslides may become leaky or sealed by deformation, potentially yielding misleading water-level readings.

REFERENCES

Bednarczyk, Z., 2015. Landslide monitoring and on-line early warning methods based on geological engineering investigations in the Beskid Niski and Beskid Średni Mountains (in Polish with English summary). Przegląd Geologiczny, **63**: 1220–1239.

Bober, L., Thiel, K., Zabuski, L., 1997. Zjawiska osuwiskowe w Polskich Karpatach Fliszowych. Geologiczno-inżynierskie właściwości wybranych osuwisk (in Polish). Wydaw. Instytutu Budownictwa Wodnego, PAN, Gdańsk.

Bromowicz, J., Gucik, S., Magiera, J., Moroz-Kopczyńska, M., Nowak, T.W., Peszat, C., 1976. The Carpathian sandstones, their significance as materials and perspectives of their utilization (in Polish with English summary). Geologia, **2**: 3–95.

Caine, N., 1980. The rainfall intensity-duration control of shallow landslides and debris flows. Geografiska Annaler, **62**: 23–27; https://doi.org/10.2307/520449

Cała, M., 2009. Osuwiska w Polsce i na świecie (in Polish). Nowoczesne Budownictwo Inżynieryjne, **3**: 68–74.

Cruden, D.M.,Varnes, D.J.,1996. Landslide Types and Processes. Transportation Research Board, U.S. National Academy of Sciences, Special Report, **247**: 36–75.

Gil, E., 1997. Meteorological and hydrological conditions of landslides in the Polish Flysch Carpathians. Studia Geomorphologica Carpatho-Balcanica, **30**: 143–158.

Gil, E., Długosz, M., 2006. Threshold values of rainfalls triggering selected deep-seated landslides in the Polish Flysch Carpathians. Studia Geomorphologica Carpatho-Balcanica, **40**: 21–43.

Gil, E., Zabuski, L., Mrozek, T., 2009. Hydrometeorological conditions and their relations to landslide processes in the Polish Flysch Carpathians (an example of Szymbark area). Studia Geomorphologica Carpatho-Balcanica, **43**: 127–143.

Golonka, J., Vašiček, Z., Skupien, P., Waśkowska-Oliwa, A., Krobicki, M., Cieszkowski, M., Ślączka, A., Słomka, T., 2008. Litostratigraphy of the Upper Jurassic and Lower Cretacous deposits of the western part of the Outer Carpathians (discussion proposition) (in Polish with English summary). Geologia, **34**: 9–31.

Gorczyca, E., 2004. Przekształcanie stoków fliszowych przez procesy masowe podczas katastrofalnych opadów (dorzecze Łososiny) (in Polish). Wydaw. Uniwersytetu Jagiellońskiego, Kraków.

Grabowski, D., Przybycin, A., 2010. Działania resortu środowiska w zakresie systemu osłony przeciwosuwiskowej w Polsce (in Polish). Przegląd Geologiczny, **58**: 941–945.

Guzetti, F., Perucacci, S., Rossi, M., Stark, C.P., 2008. The rainfall intensity-duration control of shallow landslides and debris flows: update. Landslides, **5**: 3–17; https://doi.org/10.1007/s10346-007-0112-1

Handwerger, A.l., Roering, J.J., Schmidt, D.A., 2013. Controls on the seasonal deformation of slow-moving landslides. Earth and Planetary Science Letters, **377–378**: 239–247; https://doi.org/0.1016/j.epsl.2013.06.047

Hu, X., Wang, T., Pierson, T.C., Lu, Z., Kim, J., Cecere, T.H., 2016. Detecting seasonal landslide movement within the Cascade landslide complex (Washington) using time-series SAR imagery. Remote Sensing of Environment, **187:** 49–61; https://doi.org/10.1016/j.rse.2016.10.006

Książkiewicz, M., 1953. Karpaty fliszowe między Olzą a Dunajcem (in Polish). Regionalna geologia Polski, **1**: 305–362.

Leszczyński, S., 1981. Ciężkowice Sandstones of the Silesian Unit in Polish Carpathians: a study of coarse-clastic sedimentation in deep-water (in Polish with English summary). Annales de la Société Géologique de Pologne, **51**: 435–502.

Marciniec, P., Laskowicz, I., Zimnal, Z., Grabowski, D., Rączkowski, W., 2015. The issues of landslides in the activities of the Geological Survey and public administration units (in Polish with English summary). Przegląd Geologiczny, **63**: 1364–1372.

Marciniec, P., Granoszewski, W., Zimnal, Z., 2019. Landslide on the slopes of Mt. Magura Witowska (Podhale) (in Polish with English summary). Przegląd Geologiczny, **67**: 405–413.

Mrozek, T., Bochenek, W., Gil, E., Rączkowski, W., Wójcik, A., Zabuski, L., 2006. Zintegrowane badania osuwiskowe w rejonie Szymbarku, Beskid Niski – na przykładzie projektu "Alarm" w 5. Programie Ramowym Unii Europejskiej. Zintegrowany Monitoring Środowiska Przyrodniczego, Funkcjonowanie i monitoring geoekosystemów Polski w warunkach narastającej antropopresji (in Polish). Biblioteka Monitoringu Środowiska: 121–134.

Nescieruk, P., Rączkowski, W., 2012. Monitoring wgłębny osuwisk karpackich (in Polish). In: Geologia jedna?! – II Polski Kongres Geologiczny, Warszawa, 17–19.09.2012 r. Abstrakty: 63–67. WG UW, PTG, Warszawa.

Nowak, W., 1973. Karpaty zewnętrzne (fliszowe) (in Polish). In: Budowa geologiczna Polski. Tom **1** Stratygrafia, część 2 Mezozoik (ed. S. Sokołowski): 464–467. Wydaw. Geol., Warszawa.

Paul, Z., 1991. Szczegółowa Mapa Geologiczna Polski w skali 1:50 000, arkusz Grybów (in Polish). Państwowy Instytut Geologiczny, Warszawa.

Paul, Z., 1993. Objaśnienia do Szczegółowej Mapy Geologicznej Polski w skali 1:50 000, arkusz Grybów (in Polish). Państwowy Instytut Geologiczny, Warszawa.

Pazdro, Z., Kozerski, B., 1990. Hydrogeologia ogólna (in Polish). Wydaw. Geol., Warszawa.

Perski, Z., Wojciechowski, T., 2022. Monitoring the dynamics of landslide surface movements under conditions of variable groundwater level with the use of radar reflectors (in Polish with English summary). Przegląd Geologiczny, **70**: 661–670. https:/doi.org/10.7306/2022.20

Perski, Z., Nescieruk, P., Wojciechowski, T., 2019. Landslide hazard to water reservoirs in the Carpathians (in Polish with English summary). Przegląd Geologiczny, **67**: 332–338.

Rączkowski, W., Mrozek, T., 2002. Activating of landsliding in the Polish Flysch Carpathians by end of the 20th century. Studia Geomorphologica Carpatho-Balcanica, **36**: 91–111

Ryłko, W., Paul, Z., 2014. Szczegółowa Mapa Geologiczna Polski w skali 1:50 000, arkusz Kalwaria Zebrzydowska (in Polish). Państwowy Instytut Geologiczny – PIB, Warszawa.

Solon, J., Borzyszkowski, J., Bidłasik, M., Richling, A., Badora, K., Balon, J., Brzezińska-Wójcik, T., Chabudziński, Ł., Dobrowolski, R., Grzegorczyk, I., Jodłowski, M., Kistowski, M., Kot, R., Krąż, P., Lechnio, J., Macias, A., Majchrowska, A., Malinowska, E., Migoń, P., Myga-Piątek, U., Nita, J., Papińska, E., Rodzik, J., Strzyż, M., Terpiłowski, S., Ziaja, W., 2018. Physico-geographical mesoregions of Poland: Verification and adjustment of boundaries on the basis of contemporary spatial data. Geographia Polonica, **91:** 143–170.

Starkel, L., 1996. Geomorphic role of extreme rainfall in the Polish Carpathians. Studia Geomorphologica Carpatho-Balcanica, **30**: 21–38.

Szymakowska, F., 1966. Outliers of the Magura nappe in the Jasło area and their relation with the Fore-Magura series (in Polish with English summary). Annales de la Société Géologique de Pologne, **36**: 41–63.

Szymakowska-Birkenmajer, F., Jasionowicz, J., Wójcik, A., 2014. Szczegółowa Mapa Geologiczna Polski w skali 1:50 000, ark. Frysztak (in Polish). Państwowy Instytut Geologiczny, Warszawa.

Thiel, K. (ed.), 1989. Kształtowanie fliszowych stoków karpackich przez ruchy masowe na przykładzie badań na stoku Bystrzyca w Szymbarku (in Polish). Wydaw. Instytutu Budownictwa Wodnego, PAN, Gdańsk.

Warmuz, B., Nescieruk, P., 2019. The dynamics of displacements of selected landslides in the Carpathians (in Polish with English summary). Przegląd Geologiczny, **67**: 326–331.

Wasiluk, R., Gaździcka, E., 2018. Szczegółowa Mapa Geologiczna Polski w skali 1:50 000, ark. Krzywcza (in Polish). Państwowy Instytut Geologiczny – PIB, Warszawa.

Wojciechowski, T., Borkowski, A., Perski, Z., Wójcik, A., 2012. Airborne laser scanning data in landslide studies at theexample of the Zbyszyce landslide (Outer Carpathians). Przegląd Geologiczny, **60**: 95–102.

Wójcik, A., Wojciechowski, T., 2016. Landslides as one of the most important elements of geological hazards in Poland (in Polish with English summary). Przegląd Geologiczny, **64**: 701–709.

Wójcik, A, Zimnal, Z., 1996. Landslides along the San Valley between Bachórzec and Rzeczpol (The Carpathians, the Carpathian Foredeep) (in Polish with English summary). Biuletyn Państwowego Instytutu Geologicznego, **376**: 77–91.

Wójcik, A., Jasionowicz, J., Szymakowska, F., 1992. Szczegółowa Mapa Geologiczna Polski w skali 1:50 000, ark. Jasło (in Polish). Państwowy Instytut Geologiczny, Warszawa.

Wójcik, A., Jasionowicz, J., Szymakowska, F., 1993. Objaśnienia do Szczegółowej Mapy Geologicznej Polski w skali 1: 50 000, ark. Jasło (in Polish). Państwowy Instytut Geologiczny, Warszawa.

Wójcik, A., Czerwiec, J., Krawczyk, M., 2016. Szczegółowa Mapa Geologiczna Polski w skali 1:50 000, ark. Limanowa (in Polish). Państwowy Instytut Geologiczny – PIB, Warszawa.

Wójcik, A., Czerwiec, J., Krawczyk, M., 2017. Objaśnienia do Szczegółowej Mapy Geologicznej Polski w skali 1: 50 000, ark. Limanowa (in Polish). Państwowy Instytut Geologiczny – PIB, Warszawa.

Wójcik, A., Wojciechowski, T., Wódka, M., Kaczorowski, J., Kamieniarz, S., Sikora, R., Kułak, M., Karwacki, K., Warmuz, B., Perski, Z., 2020. Development of landslide research at the Polish Geological Institute (in Polish with English summary). Przegląd Geologiczny, **68**: 356–363.

Zabuski, L., 2004. Prediction of the slope movements on the base of inclinometric measurements and numerical calculations. Polish Geological Institute Special Papers, **15**: 29–37.

Zabuski, L., Gil, E., Bochenek, W., 2004. Interdependence between groundwater level and displacement of the landslide slope. Polish Geological Institute Special Papers, **15**: 39–42.

Zabuski, L., Wójcik, A., Gil, E., Mrozek, T., Rączkowski, W., 2009. Landslide processes in a flysch massif – case study of the Kawiory landslide, Beskid Niski Mts. (Carpathians, Poland). Geological Quarterly, **53**: 317–332.

Ziętara, T., 1974. The role of landslides in modelling the Rożnów Foothills (Western Flysch Carpathians) (in Polish with English summary). Studia Geomorphologica Carpatho-Balcanica, **8:** 115–133.

Zydroń, T., Kalita-Kuźnia, K., Gryboś, M., Marcinkowska, J., 2015. Geotechnical paramaters of cover soils from valley of Siarka stream from environs of Siary and Owczary near Gorlice. Acta Scientarium Polonorum Formatio Circumiectus, **14**: 157–168.

Żytko, K., Zając, R., Gucik, S., Ryłko, W., Oszczypko, N., Garlicka, I., Nemčok, J., Eliáš, M., Menčik, E., Dvořák, J., Stránik, Z., Rakus, M., Matějowská, O., 1989. Geological Map of the Western Outer Carpathians and their Foreland. In: Geological Atlas of the Western Outer Carpathians and their Foreland (eds. D. Poprawa and J. Nemčok). Państwowy Instytut Geologiczny, Warszawa.